Biomaterials 287 (2022) 121658

Contents lists available at ScienceDirect

Biomaterials

journal homepage: www.elsevier.com/locate/biomaterials

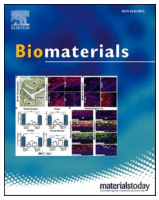

Brief exposure to directionally-specific pulsed electromagnetic fields stimulates extracellular vesicle release and is antagonized by streptomycin: A potential regenerative medicine and food industry paradigm

Craig Jun Kit Wong [a,b,c], Yee Kit Tai [a,b,c,*], Jasmine Lye Yee Yap [a,b,c], Charlene Hui Hua Fong [a,b,c], Larry Sai Weng Loo [d,e], Marek Kukumberg [f,g], Jürg Fröhlich [a,h], Sitong Zhang [a,i], Jing Ze Li [a], Jiong-Wei Wang [a,e,i,j], Abdul Jalil Rufaihah [a,g,k], Alfredo Franco-Obregón [a,b,c,e,g,i,l,**]

[a] Department of Surgery, Yong Loo Lin School of Medicine, National University of Singapore, 119228, Singapore
[b] Institute of Health Technology and Innovation (iHealthtech), National University of Singapore, 117599, Singapore
[c] Biolonic Currents Electromagnetic Pulsing Systems Laboratory (BICEPS), National University of Singapore, 117599, Singapore
[d] Institute of Bioengineering and Bioimaging, A*STAR, The Nanos, #06-01, 31 Biopolis Way, 138669, Singapore
[e] Department of Physiology, Yong Loo Lin School of Medicine, National University of Singapore, 117593, Singapore
[f] Department of Obstetrics & Gynaecology, Yong Loo Lin School of Medicine, National University of Singapore, 119228, Singapore
[g] Healthy Longevity Translational Research Programme, Yong Loo Lin School of Medicine, National University of Singapore, 119228, Singapore
[h] Fields at Work GmbH, Zurich 8032, Switzerland
[i] Nanomedicine Translational Research Programme, Centre for NanoMedicine, Yong Loo Lin School of Medicine, National University of Singapore, Singapore
[j] Cardiovascular Research Institute, National University Heart Centre Singapore, Singapore, 119074, Singapore
[k] School of Applied Sciences, Temasek Polytechnic, 529757, Singapore
[l] NUS Centre for Cancer Research, Yong Loo Lin School of Medicine, National University of Singapore, 117599, Singapore

ARTICLE INFO

Keywords:
Myokines
Extracellular vesicles
Conditioned media
Cell-based meat
TRPC1
Streptomycin

ABSTRACT

Pulsing electromagnetic fields (PEMFs) have been shown to promote *in vitro* and *in vivo* myogeneses via mitohormetic survival adaptations of which secretome activation is a key component. A single 10-min exposure of donor myoblast cultures to 1.5 mT amplitude PEMFs produced a conditioned media (pCM) capable of enhancing the myogenesis of recipient cultures to a similar degree as direct magnetic exposure. Downwardly-directed magnetic fields produced greater secretome responses than upwardly-directed fields in adherent and fluid-suspended myoblasts. The suspension paradigm allowed for the rapid concentrating of secreted factors, particularly of extracellular vesicles. The brief conditioning of basal media from magnetically-stimulated myoblasts was capable of conferring myoblast survival to a greater degree than basal media supplemented with fetal bovine serum (5%). Downward-directed magnetic fields, applied directly to cells or in the form of pCM, upregulated the protein expression of TRPC channels, markers for cell cycle progression and myogenesis. Direct magnetic exposure produced mild oxidative stress, whereas pCM provision did not, providing a survival advantage on recipient cells. Streptomycin, a TRP channel antagonist, precluded the production of a myogenic pCM. We present a methodology employing a brief and non-invasive PEMF-exposure paradigm to effectively stimulate secretome production and release for commercial or clinical exploitation.

* Corresponding author. Department of Surgery, Yong Loo Lin School of Medicine, National University of Singapore, NUHS Tower Block Level 8, 1E Kent Ridge Road, 119228, Singapore.
** Corresponding author. Department of Surgery, Yong Loo Lin School of Medicine, National University of Singapore, NUHS Tower Block Level 8, 1E Kent Ridge Road, 119228, Singapore.
E-mail addresses: surtaiyk@nus.edu.sg (Y.K. Tai), suraf@nus.edu.sg (A. Franco-Obregón).

https://doi.org/10.1016/j.biomaterials.2022.121658
Received 13 June 2022; Accepted 24 June 2022
Available online 6 July 2022

1. Introduction

Our largest tissue mass, skeletal muscle has evolved to play a fundamental role in systemic regeneration and metabolic balance. This aspect of muscle function is largely mediated via the actions of its secretome, consisting of a myriad of regenerative, metabolic, anti-inflammatory and immunity-boosting factors released into the systemic circulation as either individual [1,2] or vesicle encapsulated [3–5] components. In response to energy metabolism, such as that required to initiate and sustain exercise, muscle upregulates the production and release of blood-borne soluble factors, collectively known as myokines [1,2,6,7]. PGC-1α-dependent transcriptional co-activation of the genes involved in mitochondrial homeostasis [8,9] instigate the myokine response [10,11], whereas extracellular calcium entry [12] as well as mitochondrial respiration [9] and exercise [5] stimulate muscular extracellular vesicle (EV) release. These two aspects of the secretome are not mutually exclusive, but are activated in parallel by transduction pathways activated by exercise that are common to both limbs of the response [9,13]. Importantly, these muscular secretome responses are largely uncoupled in individuals that are inactive, sarcopenic, or otherwise too frail to exercise, with devastating metabolic and inflammatory repercussions [14–16]. Most conventional pre-habilitative and post-habilitative measures in the elderly and frail are an attempt to reengage these essential muscular responses for improved physiological resilience [17,18]. The food industry is also attentive to the development of methods to effectively enhance the production and provision of the muscle secretome [19] as approximately one-fifth of the world's protein source originates from skeletal muscle either in the form of animal-based meat [20], or more recently as cultured meat [21,22].

Brief exposure (10 min) to low amplitude (<2 mT) and low energy (Hz-kHz) pulsing magnetic fields (PEMFs) has been shown to stimulate myogenesis and mitochondrial respiration in cells [23] and in mice [24]. Magnetic enhancements of both *in vitro* and *in vivo* myogenesis were associated with PGC-1α transcriptional co-activation of mitochondriogenesis and mitohormetic survival adaptations. A key player in these magnetic mitohormetic responses was the Transient Receptor Potential Canonical 1 (TRPC1) calcium-permeable channel whose expression and function were required to elicit magnetically-stimulated chondrogenesis [25], neurogenesis [26] and myogenesis [23,24]. TRPC1 reintroduction was also shown to be necessary and sufficient to reinstate magnetically-induced mitochondrial respiration and enhanced myogenesis in a CRISPR/Cas9 TRPC1-knockdown skeletal muscle cell line [27]. Analogous magnetic stimulation was capable of activating the secretome response of mesenchymal stem cells to promote *in vitro* chondrogenesis and improve survival following induced inflammation [28] in association with TRPC1 expression [25]. Given the accepted interdependency between mitochondrial respiration and secretome response [8–11], magnetic stimulation of mitochondrial respiration in muscle cells [23] should result in secretome-dependent enhancement of *in vitro* myogenesis.

In this study, we investigated the potential of analogously brief exposure to low-energy PEMFs to promote *in vitro* myogenesis by eliciting the secretome response. Our main objective was to elucidate the magnetic and basic pharmacological requirements conferring secretome activation for the best myogenic outcome. Another objective of the study was to investigate the possibility of exogenous serum-free survival of muscle cells when provided conditioned media from PEMF-exposed muscle cells. Our analyses were predominantly conducted with the murine C2C12 muscle cell line, and validated with an immortalized primary porcine myoblast cell line. PEMF directionality turned out to be a major determinant in the secretome response that is rarely taken into consideration in existing studies [29]. Moreover, the presence of streptomycin, conventionally used in tissue culture paradigms, was found to preclude the ability of the magnetic fields to activate the cell secretome and consequently, myogenesis [23]. As a consequence of the above commonly overlooked caveats, field exposure duration used in this study is much briefer (10 min applied once) than those typically employed in published studies (hours per week) [29].

2. Materials and methods

2.1. C2C12 cell culture and chemical reagents

C2C12 mouse skeletal myoblasts were obtained from American Type Culture Collection (ATCC; LGC Standards, Teddington, United Kingdom) and cultured in Dulbecco's Modified Eagle Medium (DMEM) (Thermo Fisher Scientific, Waltham, MA, USA) containing 10% fetal bovine serum (FBS) (Cytiva, Marlborough, USA), and maintained in a humidified incubator with 5% CO_2. Cells were passaged every 48 h to maintain them below 40% confluence, unless otherwise explicitly stated. Myoblasts were seeded into tissue culture dishes/flasks at 3000 cells/cm^2 [23], unless otherwise explicitly stated. Twenty-four hours later the plates were exposed to pulsed electromagnetic fields (PEMFs). Cell number in each well of a 6-well plate was determined using enzymatic dissociation with TrypLE Express Enzyme (Thermo Fisher Scientific, Waltham, MA, USA), followed by the standard trypan blue exclusion method, and counted with a hemocytometer.

2.2. Porcine myoblast culture and chemical reagents

Passage 17 (P17) porcine myoblasts were grown in growth media consisting of Nutrient Mixture F-10 Ham (Merck, Germany, #N6635), 15% FBS (Hyclone, #SV30160·03HI), 1% penicillin-streptomycin (Sigma, #P4333) and 10 ng/ml Fibroblast Growth Factor 2 (FGF2) (Invitrogen, Carlsbad, CA, USA, PHG0360). Upon reaching 80% confluency in a 10 cm plate, porcine myoblasts were trypsinized using 3 ml of TrypLE (Thermo Scientific, #12605010) and incubated at 37 °C for 5 min. Afterwards, 10 ml of porcine full growth media was added to neutralize the TryPLE and the cell suspension was centrifuged at 1500 rpm for 5 min to obtain the cell pellet. The cell pellet was then resuspended in 5 ml of fresh porcine growth media without the addition of penicillin-streptomycin. Cell counting was performed using a hemocytometer and a total of 60,000 cells were seeded into each well of 6-well plates containing 2 ml of myoblast full growth media without penicillin-streptomycin. The porcine myoblasts were then left to incubate overnight at 37 °C in a standard tissue culture incubator.

2.3. Pulsed electromagnetic fields (PEMFs) exposure

The PEMF signal used in this study has been described and myogenically characterized in previous studies [23,24]. Briefly, the employed PEMF devices produce spatially homogeneous, time-varying magnetic fields, consisting of barrages of 20× 150 μs on and off pulses for 6 ms at a repetition frequency of 15 or 50 Hz. The magnetic flux density plateaued at a predetermined amplitude of 1.5 mT within ~50 ms (~17 T/s). As previously described [30], all tissue culture flasks, dishes or tubes were placed within a region of greatest magnetic field uniformity within which the entirety of the vessel is exposed evenly to the traversing magnetic field lines. All PEMF-treated samples were compared with time-matched control samples (0 mT) that were manipulated in the same way as the experimental samples, including placement into the PEMF-generating apparatus for the designated time, except that the apparatus was not set to generate a magnetic field. All magnetically-stimulated samples in this study were exposed once for a duration of 10 min to 1.5 mT amplitude PEMFs of different field line directionalities.

2.4. Field directionality

Employed in this study were an *in vitro* coil system (Coil 1) [23], animal coil system (Coil 2) (Fields at Work, Zürich), human leg coil system (Coil 3) (FLEX LTD. Singapore), human arm coil system (Coil 4)

(HOPE Technik PTE. LTD. Singapore) and human breast cancer coil (Coil 5) (FLEX LTD. Singapore) [31]. All coil systems were designed to generate analogous magnetic fields as described above. PEMF Coil systems 1 and 2 were designed with an in-built capability to electronically switch field directionality, upwards or downwards. Briefly, the directionality of field exposure is a function of the direction of the current flowing through the field generating coil sub-assemblies. By changing the direction of the current flow, the field direction can be inverted. A polarity-switching H-bridge was implemented to allow for the switching of field directionality by reversing the signal current applied to the coil system. Changes in magnetic field directionality with PEMF coil systems 3, 4 and 5 were accomplished by manually flipping the orientation of the coil system relative to the culture flask placed within the lumen of the coils. Field uniformity produced by the distinct coil systems was routinely validated using an ExpoM-ELF (Fields at Work, Zürich) low-frequency magnetic fields exposure meter. Magnetically-induced C2C12 murine muscle cell proliferation enhancement was similar in magnitude with all PEMF devices.

Myoblast cultures were exposed to one or more of the following conditions: **1**) unexposed 0 mT; **2**) 1.5 mT exposure in the horizontal direction; **3**) 1.5 mT exposure in the downward direction and; **4**) 1.5 mT exposure in the upward direction. Culture dishes were placed within the indicated coil system in the intended horizontal (flat) position with the magnetic field lines oriented either parallel or perpendicular to the long axis of the plate, unless otherwise explicitly stated (see next).

2.5. Interaction between flask orientation and magnetic field directionality

Cells were seeded at 3000 cells/cm^2 into T25 flasks and 24 h later exposed to 1.5 mT amplitude PEMFs. The directionality of the PEMF field lines applied to the flasks were either: **1**) horizontal; **2**) downward or; **3**) upward direction. To study the interplay between flask orientation and magnetic field direction, culture T25 flasks were exposed to PEMFs of the above directionalities while either lying in the prescribed horizontal position or in a standing upright (vertical) position. While in the standing orientation the flask and cells were temporarily filled with media to the brim to prevent the adhered cells from drying out while the flasks were in the upright position. Immediately after PEMF exposure, excess media was removed from the standing flasks, leaving only 5 ml media in each flask to nurture cell growth while in a conventional horizontal position within a tissue culture incubator. Unexposed flasks represented the 0 mT control scenarios and were in either horizontal or standing positions as indicated in the applicable figure legend. Cell number was determined after 24 h of growth.

2.6. PEMF-conditioned media and washout experiments in adherent cultures

Twenty-four hours post-cell seeding, donor cultures grown in flasks were exposed to PEMFs of the indicated direction for 10 min or placed within the unpowered coil system for 10 min to serve as the control condition. CM from the donor cells was collected 6 h post-conditioning and given to age-matched naïve recipient cultures (scenario 1). For CM washout experiments (scenario 2), CM from PEMF-exposed cells were removed 1 h post-PEMF exposure and replaced with age-matched media from unexposed sister cultures. Cell counts were performed on the recipient cultures 24 h following the transfer of CM (scenario 1) or the delivery of age-matched naïve media (scenario 2).

2.7. Cell suspension experiments and PEMF-conditioned media collection

For the examination of PEMF-exposed cell suspension and their associated CM, cells in suspension were generated by enzymatically dissociating adherent cells from T75 flasks and resuspending them into 24 ml of growth media (DMEM + 10% FBS) at a concentration of 35,000 cells/ml media. The cell suspension was then subdivided into 4 independent 50 ml conical tubes and exposed to either one of these conditions **1)** 0 mT; **2)** 1.5 mT horizontal direction; **3)** 1.5 mT downwards direction; or **4)** 1.5 mT upwards direction. The cells were then plated into a 6-well plate at a density of 3000 cells/cm^2 and allowed to grow for 24 h before counting.

For the generation of CM from different cell suspension densities, cells resuspended in 12 ml of complete DMEM (1X cell density) were exposed to PEMFs and allowed to recover in a standard tissue culture incubator for 30 min and to condition the bathing media. The cell suspension was then centrifuged at 1200 rpm for 5 min and the supernatant (CM) was given to pre-plated naïve recipient cultures and allowed to grow for 24 h later before counting. For 5X experiments, the number of cells in suspension was 5-fold greater than the 1X density, reconstituted in the same 1X volume of complete media that was later used to generate CM to be given to pre-plated naïve cells prior to counting. The final concentration of cells for the 1X and 5X conditions were 15,000/ml and 75,000/ml, respectively.

2.8. Streptomycin treatments

For experiments with adherent cultures, streptomycin (0.1 mg/ml; Merck, Germany) was added directly to the cell culture media 2 h before PEMF exposure. Six hours following active or sham exposure, the conditioned media was harvested from donor cultures and given to recipient cultures in replacement for their existing media and allowed to grow for 24 h before cell enumeration. For cell suspension experiments, streptomycin (0.1 mg/ml) was added at the time of cell resuspension, immediately followed by PEMF exposure. The cells were then allowed to recover in a standard tissue culture incubator for 30 min before centrifugation at 1200 rpm for 5 min prior to the collection of the supernatant to be used as conditioned media on pre-plated naïve recipient cultures. The recipient cultures were allowed to grow for 24 h before cell counting.

2.9. Western blot analysis of whole cell lysates

Protein extraction was performed using RIPA lysis buffer containing 50 mM NaCl, 1 mM EDTA, 50 mM Tris-HCl, 1% Triton X-100, 0.05% SDS, EDTA-free 1X protease inhibitor cocktail (Nacalai Tesque Inc., Japan), 1X PhosSTOP™ phosphatase inhibitor (Merck, Germany) and 0.1% sodium deoxycholate (Merck, Germany). Whole cell lysates were collected using a cell scraper and incubated at 4 °C for 30 min before being spun at 12,000 rpm for 15 min at 4 °C. Protein concentration was determined using Pierce BCA Protein Assay Kit (Thermo Fisher Scientific, Waltham, MA, USA). Whole cell lysates were prepared in 4X Laemmli buffer with added β-mercaptoethanol (Bio-Rad Laboratories and Sigma Life Science, USA, respectively) and were boiled at 95 °C for 5 min. 20–25 μg of proteins from the whole-cell lysates were resolved using denaturing and reducing SDS-PAGE and transferred to PVDF membrane (Thermo Fisher Scientific, Waltham, MA, USA). The antibodies and dilution factors used are listed in Table 1.

2.10. Reactive oxygen species measurements

For the determination of ROS in cells directly exposed to PEMFs, cells were seeded in black-walled clear bottom 96-well plates (Corning, New York, USA) at a density of 3000 or 6000 cells per well with 8 replicates per condition. 24 h post-seeding, the cells were rinsed twice with warm phenol-free and FBS-free (PFSF) DMEM (Thermo Fisher Scientific, Waltham, MA, USA) and incubated with 5 μM of CM-H2DCFDA (Thermo Fisher Scientific, Waltham, MA, USA) in PFSF DMEM for 30 min. The individual 96-well plates were exposed to PEMFs at the indicated direction for 10 min and left in the standard culture incubator for 10 min. The media containing CM-H2DCFDA was replaced with PSFS DMEM before proceeding with the ROS measurement using a Cytation 5

Table 1
List of antibodies, vendors and employed dilution factors.

Protein target and catalogue number	Vendor, Country	Dilution Factor
Cyclin-dependent kinase inhibitor (P21) (sc-6246)	Santa Cruz Biotechnology, Texas, USA	1:300
Cyclin B1 (CB1) (CST 4138)	Cell Signaling Technology, Massachusetts, USA	1:1000
Cyclin D1 (CD1) (sc-8396)	Santa Cruz Biotechnology, Texas, USA	1:300
Desmin (ab907)	Merck Millipore, USA	1:1000
HTRA serine peptidase 1 (HTRA1) (55011-1-AP)	Proteintech, Chicago, USA	1:1000
Transient receptor potential canonical 1 (TRPC1) (sc-133,076)	Santa Cruz Biotechnology, Texas, USA	1:300
Transient receptor potential canonical 3 (TRPC3) (sc-514,670)	Santa Cruz Biotechnology, Texas, USA	1:300
Transient receptor potential canonical 6 (TRPC6) (sc-515,837)	Santa Cruz Biotechnology, Texas, USA	1:300
Transient receptor potential cation channel subfamily M member 7 (TRPM7) (ACC-047)	Alomone, Israel	1:200
Myoblast determination protein 1 (MyoD) (sc-71626)	Santa Cruz Biotechnology, Texas, USA	1:300
Myogenin (MyoG) (immunofluorescence and western blotting) (sc-12732)	Santa Cruz Biotechnology, Texas, USA	1:20 (IF), 1:300 (WB)
Glyceraldehyde-3-phosphate dehydrogenase (GAPDH) (60,004-1-lg)	Proteintech, Chicago, USA	1:10,000
Phospho-JNK (sc-6254) and Total JNK (sc-7345)	Santa Cruz Biotechnology, Texas, USA	1:300
Phospho-ERK (sc-7383) and Total ERK (s-514,302)	Santa Cruz Biotechnology, Texas, USA	1:300
CD9 (sc-13118)	Santa Cruz Biotechnology, Texas, USA	1:300
Calnexin (ab133615)	Abcam, Cambridge, UK	1:1000
CD9 (flow cytometry) (48-0091-82)	Life Technologies, USA	1:20
CD81 (flow cytometry) (MA528658)	Life Technologies, USA	1:20

microplate reader (BioTek, Vermont, USA) at Ex/Em: 492/520 nm, hourly for up to 4 h.

For the determination of ROS in cells treated with conditioned media, the conditioned media was collected from donor suspension cells 30 min post PEMF exposure in the field direction as indicated. Pre-plated cells in 96-well plates were incubated with conditioned media for 2 h before they were then rinsed twice with PFSF DMEM and incubated with CM-H2DCFDA. The subsequent steps were carried out according to the protocol as described above.

2.11. Myotube differentiation, fusion index quantification and confocal microscopy

Myotubes were generated using C2C12 myoblasts seeded at 8000 cells/cm^2 in DMEM supplemented with 10% FBS. Differentiation media (DMEM containing 2% horse serum) was added to day 4 and day 6 myoblast cultures for analysis on day 8 [23]. To investigate the effect of pCM on the differentiation of myoblasts, a 5X concentration of myoblasts were resuspended in 11 ml of basal DMEM. Following PEMF exposures, the suspended myoblasts were allowed to condition the media for 1 h in a standard tissue culture incubator at 37 °C. The cell suspensions were then centrifuged at 1200 rpm for 5 min; 9.8 ml of the supernatant was supplemented with 200 μl of horse serum (2%) before adding to myoblast cultures (day 4 of culture) to promote differentiation. This step was repeated on day 6 of culture. Hematoxylin and Eosin staining was performed on the day 8 myotubes on coverslips for the quantification of fusion index [23]. Immunofluorescence staining was done according to the previously described protocol [31]. Briefly, myotubes grown on glass coverslips were permeabilized, blocked and stained with myogenin antibody overnight. The cells were subsequently stained with anti-mouse Alexa Fluor 594 antibody (1:1000; Thermo Fisher Scientific, Waltham, USA) for 1 h followed by DAPI staining (1 mg/ml; Sigma Aldrich, USA) for 1 min. The stained cells were mounted onto glass slides with Vectashield Antifade Mounting Medium (Vector Laboratories, Newark ,CA, USA). Confocal imaging was done using an Olympus FV1000 microscope. The myogenin nuclear/cytoplasmic intensity ratio was determined using the ImageJ line plot profile function by dividing the average myogenin nuclear intensity by the cytoplasmic intensity of myotubes.

2.12. Multiplexed proteomic analysis of C2C12-derived secretome

Conditioned media from C2C12 cells in suspension (375,000 cells/ml) was collected 1 h after a 10-min PEMF exposure by centrifugation at 1200 rpm for 5 min. The secretome was analyzed using a mouse-specific Myokine Magnetic Bead Panel (Milliplex Map Kit; MMYOMAG-74 K, Merck Millipore, USA) to simultaneously quantify the presence of the following analytes: Erythropoietin (EPO), Fibroblast growth factor (FGF21), Fractalkine/CX3CL1, Follistatin-like Protein 1 (FSTL-1), Interleukin 6 (IL-6), Interleukin 15 (IL-15), Irisin, Leukemia Inhibitory Factor (LIF), Myostatin (MSTN)/GDF8, Oncostatin M (OSM), Osteocrin/Muscurin (OSTN), Osteonectin (SPARC) and Brain-Derived Neurotrophic Factor (BDNF). The immunoassay procedure was performed according to the manufacturer's workflow and subsequently analyzed on the Luminex 200 System (Thermo Fisher Scientific, Waltham, USA).

2.13. Isolation of PEMF-exposed C2C12-derived EVs

Prior to PEMF exposure, C2C12 cells in suspension were given fresh DMEM supplemented with exosome-depleted FBS (5%). After PEMF exposure, the conditioned media from C2C12 suspension cells were centrifuged at 1200 g for 5 min followed by centrifugation at 10,000 g for 30 min for the removal of microvesicles. The supernatant was next ultra-centrifuged at 120,000 g for 2 h using Quick-Seal Round-Top ultracentrifuge tubes on Optima XPN-100 Ultracentrifuge (Beckman Coulter, USA) at 4 °C to isolate EVs. EVs were resuspended in 300 μl of basal DMEM; 100 μl of the exosome suspension was given to each of three technical replicates of pre-plated C2C12 myoblasts in 2 ml of fresh growth media. The corresponding supernatants were similarly given to pre-seeded cells to assay for the presence of soluble factors. Recipient cells were allowed to grow for 24 h before cell enumeration using the Trypan Blue assay.

2.14. Protein characterization of C2C12-derived EVs using western analysis and flow cytometry

Isolation of EVs from C2C12 myoblasts in suspension was performed using the ultra-centrifugation method as described above. The exosome pellets were either resuspended in 200 μl RIPA buffer or 50 μl PBS containing 0.2% BSA for western analysis or flow-cytometry, respectively. For western analysis, equal volumes of samples in 4X loading buffer were resolved on 12% SDS-PAGE gels to determine the expressions of exosomes in the EV fraction and cytoplasmic proteins in the whole cell lysate. For flow cytometry, samples were stained with fluorescent-labeled CD81 and CD9 at room temperature for 1 h in the dark before being diluted 200X in PBS for subsequent analysis using a Cytoflex S Flow Cytometer (Beckman Coulter, CA, USA).

2.15. Physical characterization of C2C12-derived EVs using TEM and NTA

EVs were morphologically characterized as previously described [32]. In brief, EVs were incubated on formvar film-coated copper grids (FF200–Cu, 200 mesh) for 10 min. Afterward, negative staining of EVs was performed by incubating the grids with 2.5% gadolinium triacetate for 2 min. Images were taken with an FEI TECNAI SPIRIT G2 transmission electron microscope (FEI Company, USA). To determine the size distribution and concentrations of EVs, samples were diluted in MilliQ water to 112 μg/ml followed by nanoparticle tracking analysis (NTA) using a NanoSight NS300TM (Malvern Instruments, Malvern, UK). All acquisitions were processed at a camera level setting of 12 or 13, and five videos were recorded for each sample.

2.16. Statistical analysis

All statistics were carried out using GraphPad Prism (Version 9) software. One-way analysis of variance (ANOVA) was used to compare the values between two or more groups supported by multiple comparisons.

3. Results

3.1. Brief PEMF exposure stimulates secretome release

As a standard protocol used for all subsequent experiments, conditioned media was collected from myoblasts after a single 10-min exposure to 1.5 mT amplitude PEMFs or sham treatment (0 mT). To elucidate potential magnetically-induced paracrine effects as previously demonstrated in primary human mesenchymal stem cells [28], naïve C2C12 myoblast cultures (recipients) were provisioned with PEMF-conditioned media (pCM) collected from PEMF-stimulated C2C12 cells (donors) and the resulting proliferative responses compared to that of directly exposed or unexposed cells (Fig. 1a). In response to pCM administration, recipient myoblasts exhibited a significant increase in proliferation of similar magnitude to that observed for directly exposed myoblasts (Fig. 1b; blue), compared to cells provided control conditioned media (cCM) or unexposed cells (Fig. 1b; red), respectively, that exhibited similar levels of growth. By contrast, removal of the bathing media from C2C12 cultures 1 h after PEMF exposure and replacing it with media harvested from age-matched naïve sister cultures (cCM) precluded the typical proliferative response induced by PEMF exposure (Fig. 1c-d), indicating an underlying paracrine basis for the effect that moreover, appears to be enacted en masse as a single replacement of media 1 h after PEMF exposure was able to annul the response.

Aligning with previous studies demonstrating TRPC1-mediated PEMF-responses in suspensions of intact cells [23,27] or cell-derived vesicles [27], we show that myoblasts in suspension (Fig. 1e) similarly responded to PEMF exposure with the production of a pCM capable of conferring proliferation enhancement to naïve myoblasts (Fig. 1f) that was similar in magnitude to the proliferative response observed when directly plating suspended cells onto tissue culture plastic after PEMF exposure (Fig. 1f). Notably, the effective conditioning of the pCM from cell suspensions in respond to only 15–30 min after PEMF exposure indicates that *de novo* biosynthesis was not required for the response and rather that the secretome pool was readily poised and immediately released upon magnetic stimulation. Moreover, responses generated from cells in suspension discount substrate-based mechanotransduction as being the underlying force instigating secretome release [33]. The ability of PEMFs to stimulate the muscle cell secretome hence appears to be a predominantly magnetic phenomenon and, by association, should be subject to modulation by parameters such as a simple change in field orientation [34].

3.2. Magnetic field directionality

Magnetic field orientation was previously shown to influence MSC-chondrogenesis [35]. In prior experiments (Fig. 1a–d), culture flasks were positioned horizontally and exposed to PEMFs whose field lines flowed in the downward direction, perpendicular to the cell's long axis. Direct exposure of myoblast cultures in the downward direction (Fig. 2a, solid blue) rendered a 50% increase in myoblasts proliferation 24 h after exposure (Fig. 2b). By contrast, changing the direction of the magnetic field from downwards to upwards (Fig. 2a, vertical blue stripes), reduced the induced proliferation response to 20% over non-exposed control cultures (Fig. 2b, red), and exposing myoblasts to magnetic fields aligned parallel to the dish, or horizontally (Fig. 2a, horizontal blue stripes), rendered the least amount of cell growth that was statistically indistinguishable from no exposure (Fig. 2b). The proliferative potencies of the magnetically-produced secretomes paralleled those of direct exposure (Fig. 2c), being greatest for pCM produced by downward magnetic field exposure (Fig. 2d, solid blue) and the least for pCM produced by horizontal exposure (Fig. 2d, horizontal blue stripes). Magnetic field exposure orthogonal to the major axes of the tissue culture flask (and cells) hence exerts greater proliferative effects, with downward exposure producing the overall strongest response. Finally, these effects appear to be largely mediated via the secretome responses of myoblasts.

The previous results might suggest that the cell symmetry contributes to magnetotransduction, such that flattened cells on a two-dimensional surface would exhibit long (in-plane of substrate) and short (orthogonal to the plane of substrate) aspects that interact differently with magnetic field direction (Supplemental Figure 1). However, if differences in cell symmetry were solely responsible for specificity to magnetic field orientation, then rounded cells in suspension (showing equal aspect ratios) would not be expected to distinguish field orientation via this criterion, much less directionality (up versus down) (Fig. 2e). Provocatively, downward field exposure (Fig. 2f, solid blue) still produced the greatest proliferative response of cells in suspension of ~50% over baseline when replated, whereas upward (Fig. 2f, vertical blue stripes) and horizontal field exposures (Fig. 2f, horizontal blue stripes) gave nearly identical responses of ~20% over unexposed controls (Fig. 2f, red). Recapitulating previous results, pCM alone (without cells) harvested from myoblasts exposed to downwardly directed magnetic fields while in suspension (Fig. 2g) produced greater proliferation enhancement (~50%) of pre-plated recipient myoblasts (Fig. 2h, solid blue) than pCM harvested from upwardly field exposed myoblasts (~20%) (Fig. 2h, blue vertical stripes). By contrast, myoblasts given unexposed cCM (Fig. 2h, solid red) or kept in their basal growth media (Fig. 2h, red hatched) (Fig. 2h) revealed analogous levels of basal proliferation, indicating that the mechanical stimulation (osmotic pressure changes and shear stresses) arising from the media transfer alone is insufficient to stimulate secretome responses. The employed experimental design assured that the secretome levels were not increasing as the result of an inadvertent increase in cell number in response to field exposure, or otherwise. This eventuality was controlled for by the 30-min conditioning of media (too brief to allow for cell division to occur) in the suspension paradigm as well as the 1X cell density condition, reflecting the identical number of cells exposed as in the adherent cultures. Finally, the enhanced proliferation conferred by downward-directed PEMF exposure, relative to upward PEMF-exposure, could be shown to be independent of the device being used (Supplemental Figure 2), indicating that technical idiosyncrasies of a particular device are not responsible for the effect as well as demonstrating the feasibility of future translation. Therefore, downwardly directed magnetic fields *per se* exert proliferative enhancement, independently of cell symmetry and are associated with selective activation of the cell secretome.

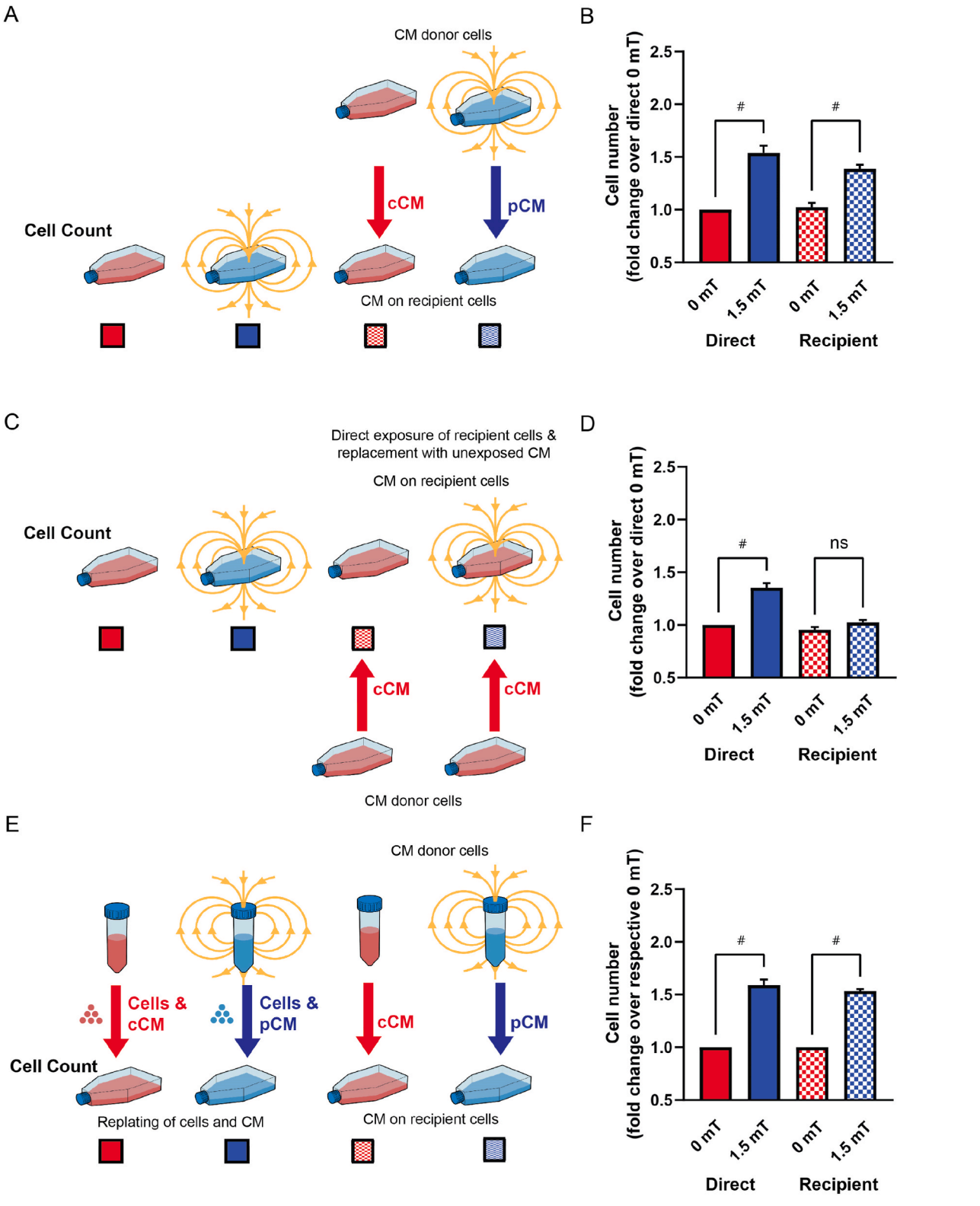

(caption on next page)

Fig. 1. Magnetic-induced proliferation enhancement can be conferred to naïve myoblasts with the provision of PEMF-conditioned media (pCM). A) Schematic depiction of the experimental paradigm for proliferation assessment under basal conditions (red) or following magnetic stimulation (blue) for myoblasts directly kept in their original bathing media (solid) or upon the transfer of the conditioned media to naïve age-matched recipient cultures (cross-hatched). **B)** Proliferation induction normalized (fold change) to the unexposed condition (solid red), as indicated. Recipient cultures were given conditioned media (CM) either from magnetically-stimulated (pCM) or unexposed (cCM) donor cultures, blue and red cross-hatched, respectively. Data represents the average of n = 14 biological replicates. **C)** Magnetic-induced proliferation enhancement could be nullified by the replacement of pCM with cCM. Depiction of proliferation assessment under basal conditions (red) or following magnetic stimulation (blue), directly (solid) or upon transfer of cCM from unexposed age-matched sister cultures (cross-hatched). **D)** Quantification of induced proliferation expressed as fold change relative to direct 0 mT (red). Hatched bars represent the values for previously exposed recipient cultures after cCM washout. Data represents the average of n = 7 biological replicates. **E)** Depiction of proliferation assessment for suspension cultures without magnetic exposure (red) or upon magnetic stimulation (blue), prior to the replating of the cells (dots) and their respective CMs into empty culture flasks (solid) or upon the delivery of the distinct CMs (without cells) to age-matched recipient cultures (hatched). **F)** Quantification of induced proliferation expressed as fold change relative to direct 0 mT. Data represents the average of n = 3 biological replicates. All magnetic exposures consisted of downward-directed PEMFs at an amplitude of 1.5 mT applied once for 10 min. Conditioned media was transferred to recipient cultures 6 h (**A**–**B**) or 30 min (**E**, **F**) following PEMF or sham exposure of donor cultures; media was removed from recipient cultures 1 h after PEMF or sham exposure and replaced with age-matched media from untreated donor sister cultures (**C**–**D**). Error bars represent the standard error of the mean, with $^{\#}p < 0.0001$, analyzed using One-Way ANOVA with Sidak's multiple comparisons test. All biological replicates were derived from the means of three technical replicates.

3.3. Streptomycin blocks magnetically-stimulated secretome enhancement

The aminoglycoside antibiotics preclude PEMF-induced myogenic responses by blocking calcium entry via TRPC1 channels, effectively interfering with the activation of NFAT/calcineurin-mediated enzymatic and transcriptional cascades involved in myogenic progression [23]. Accordingly, streptomycin added to myoblast cultures just before PEMF exposure (Fig. 3a) prevented the production of a myogenic pCM (Fig. 3b). This result reveals the potency of the PEMF-induced secretome compared to constitutive release. Analogously, streptomycin added right before PEMF exposure was also capable of equally preventing the production of a myogenic pCM from myoblasts in suspension at cell concentrations of 15,000/ml (1X) or 75,000/ml (5X) (Fig. 3c-d). A generalized cytotoxicity of streptomycin cannot underlie the inhibition of proliferation observed in the pCM scenario (blue; + Strep) as basal proliferation (red) was not reduced by cCMs containing streptomycin (red; + Strep). These combined results underscore the degree by which proliferation is enhanced by factors whose secretion was induced by brief magnetic stimulation.

3.4. Direct downward field exposure preferentially upregulates myogenic proliferation and differentiation regulator protein expression

Given previous evidence that analogous magnetic exposure stimulates myogenic proliferation and differentiation in association with TRPC1 function and expression [23], we investigated whether TRPC1 expression was regulated in parallel to secretome response by magnetic field directionality. TRPC1 protein expression in myoblasts was found to be preferentially elevated by exposure to downward PEMFs (Fig. 4a). The protein expressions of TRPC1, TRPC3, TRPC6 and TRPM7 were all also preferentially upregulated by downward magnetic fields after 24 h of growth (Fig. 4a–d). TRPC1 (Fig. 4a) and TRPC6 (Fig. 4c) demonstrated the greatest specificity for field directionality, manifested by the most significant upregulations with downward exposure, relative to upward or no exposure.

We next examined the protein expression of regulators of myogenic proliferation and differentiation in response to up or direct downfield exposure. Cyclins B1 (Fig. 4e) and D1 (Fig. 4f) were preferentially upregulated by downward fields, consistent with cell cycle progression in C2C12 muscle cells [36], and in this report associated with proliferation enhancement in response to direct downward field exposure and pCM provision. By contrast, the expression levels of p21, a cyclin-dependent kinase (CDKs) inhibitor [37], were instead reduced by downward magnetic fields and unaltered by upward field exposure (Fig. 4g). Myoblast Determination Protein 1 (MyoD) (Fig. 4h) and Myogenin (MyoG) (Fig. 4i) levels were both preferentially upregulated by downwardly directed magnetic fields consistent with early MyoD and NFAT co-transcriptional regulation of MyoG required for downstream myogenic differentiation [38], a feature shared with analogous PEMF exposure of myoblasts [23] and animals [24]. Therefore, both the proliferation and differentiation phases of myogenesis are preferentially enhanced by downward field exposure.

Interestingly, the protein levels of high-temperature requirement A1 (HtrA1) were also significantly elevated by direct downward field exposure (Fig. 4j). HtrA1 is a secreted serine protease and oxidative stress response protein that is reduced in diverse cancers and is reputed to possess tumor-suppressive properties [39,40]. Moreover, HTRA1 has been shown to sensitize cancer cells to a broad range of chemotherapies [41–44]. It is intriguing to speculate that HTRA1 may belong to the collection of reported exercise-induced myokines with anti-cancer attributes [45–48]. Muscular secretion of HTRA1 under appropriately administered magnetic stimulation may hence hold important implications for cancer management.

3.5. Downward field conditioned media preferentially upregulates myogenic proliferation and differentiation regulator protein expression

The TRPC channel family exhibits a particular predilection for growth factor regulation of function and expression, expressly TRPC1 with a general outcome of proliferation modulation [49]. Moreover, TRPC1 shows the greatest capacity to heteromultimerize with the other TRPC family members, theoretically uniting their distinct activation modes into a single channel complex [50]. To examine whether the upregulation of TRPC channels, cell cycle and myogenic proteins is the cause, or effect, of myokine release we examined their protein expression levels in recipient cells following incubation in either cCM or pCM generated in response to upward and downward field exposure of myoblasts in suspension at low (1X) and high (5X) cell densities (Fig. 5). Delivery of CM mirrored the effects of direct exposure. Similar to the preferential response of myoblasts to direct downward field exposure, TRPC1 and TRPC6 in recipient myoblasts showed the most selective responses to pCM generated from myoblasts exposed to downward fields. The protein levels of markers of cell cycle and myogenic progression showed a similar preferential upregulation in response to pCM produced by downward field exposure (Fig. 5e and f), whereas p21 protein levels were reduced by pCM of either directionality (Fig. 5g) suggesting a relative attenuation of oxidative stress [51] in response to pCM delivery compared to direct exposure of cells. HTRA1 levels were preferentially upregulated by downward pCM provision (Fig. 5i) to a greater degree than direct downward exposure (Fig. 4j). The expressional responses to pCM provision were generally more pronounced than that observed in response to direct exposure of myoblasts (cf. Fig. 4). The immediate release of existing secretome components is reasonably a major contributor to the observed cellular response to magnetic field stimulation and mechanistically aligns with the observed prompt induction of proliferation immediately after PEMF exposure (Supplemental Videos S1a and S1b) that is much too rapid to be attributed to the *de novo* synthesis of secretome elements [23].

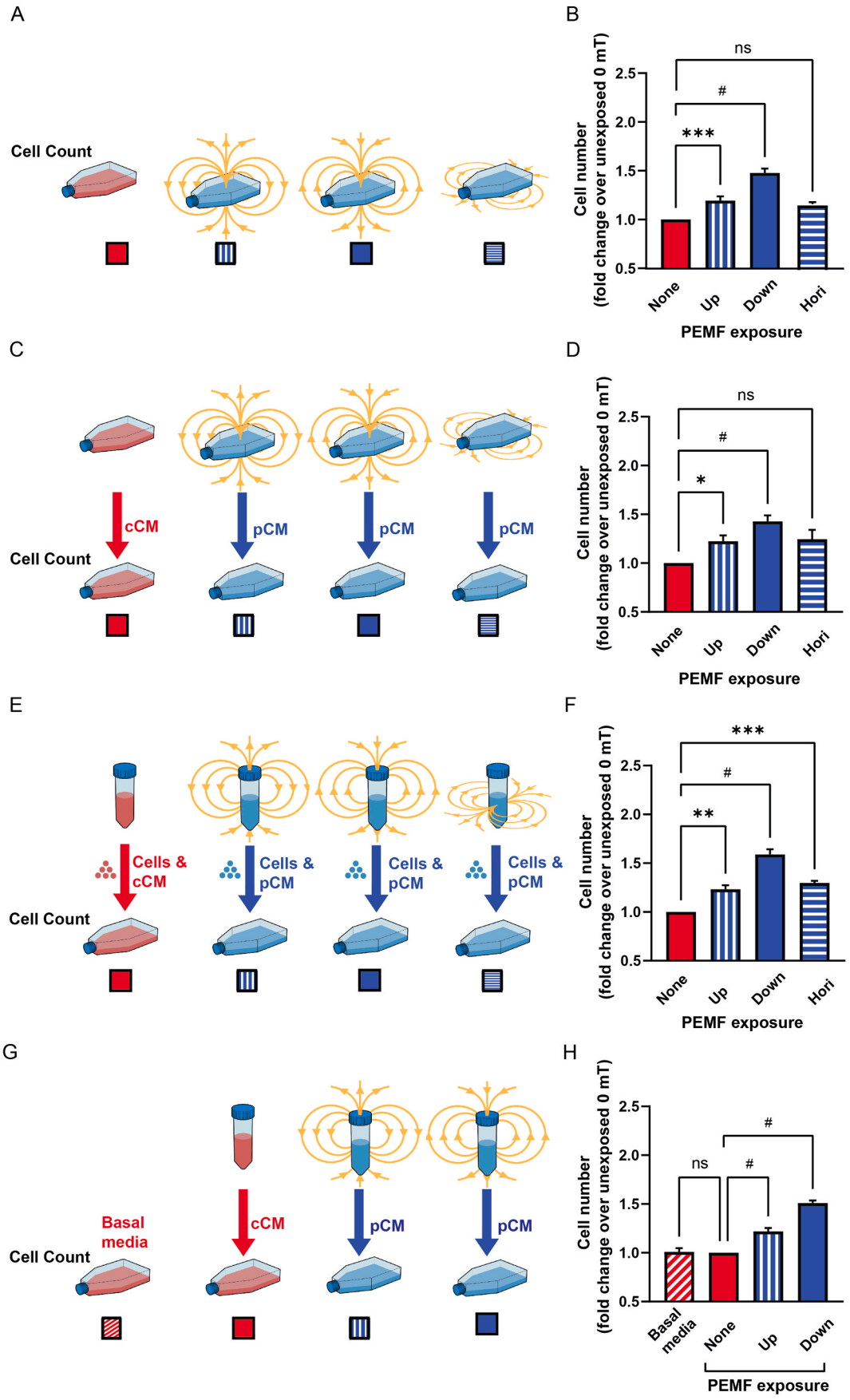

(caption on next page)

Fig. 2. Magnetic field directionality determines the efficacy of pCM. A) Schematic representation of culture flasks under basal conditions (unexposed; red) or upon direct exposure to magnetic fields (blue) of up, down or horizontal directionalities, as indicated. **B**) Quantification of induced proliferation in response to upward (vertical blue stripes), downward (solid blue) or horizontal (horizontal blue stripes) field exposure relative to unexposed cultures (red). Data represents the average of n = 3–14 biological replicates. **C)** Depiction of recipient cultures receiving cCM (red) or pCM (blue) that had been generated under analogous exposure conditions as shown in **A**. **D**) Quantification of induced proliferation in recipient cultures in response to pCM generated from donor cultures receiving upward (vertical blue stripes), downward (solid blue) or horizontal (horizontal blue stripes) field exposure relative to cultures receiving cCM (red). Data represents the average of n = 7–15 biological replicates. **E**) Schematic representation depicting cells in suspension under basal conditions (red) or upon exposure to upward (vertical blue stripes), downward (solid blue), or horizontal (horizontal blue stripes) magnetic fields before replating both the suspended cells (blue dots) and their respective conditioned-media into new culture flasks for subsequent growth assessment. **F**) Quantification of induced proliferation in response to the indicated pCMs plus cells relative to cultures receiving cCM and unexposed cells. Data represents the average of n = 3 biological replicates. **G**) Depiction of the transfer of CM (cCM or pCM) from cells in suspension to recipient cells prior to cell growth assessment. **H**) Quantification of induced proliferation in recipient cultures after receiving the indicated pCMs relative to cultures receiving cCM. Recipient cultures were either grown in their basal media (diagonal red stripes), received cCM from unexposed suspension cells (solid red), or pCM from suspension cells that were exposed to upward (vertical blue stripes) or downward (solid blue) magnetic fields. Data represents the average of n = 9 biological replicates. All biological replicates were derived from the means of three technical replicates. All magnetic exposures consisted of PEMFs at an amplitude of 1.5 mT applied once for 10 min. Error bars represent the standard error of the mean, with $^{*}p < 0.05$, $^{**}p < 0.01$, $^{***}p < 0.001$ and $^{\#}p < 0.0001$, analyzed using One-Way ANOVA with Dunnett's multiple comparisons test. "ns" indicates statistical nonsignificant differences. "None" refers to cultures given cCM or no magnetic exposure.

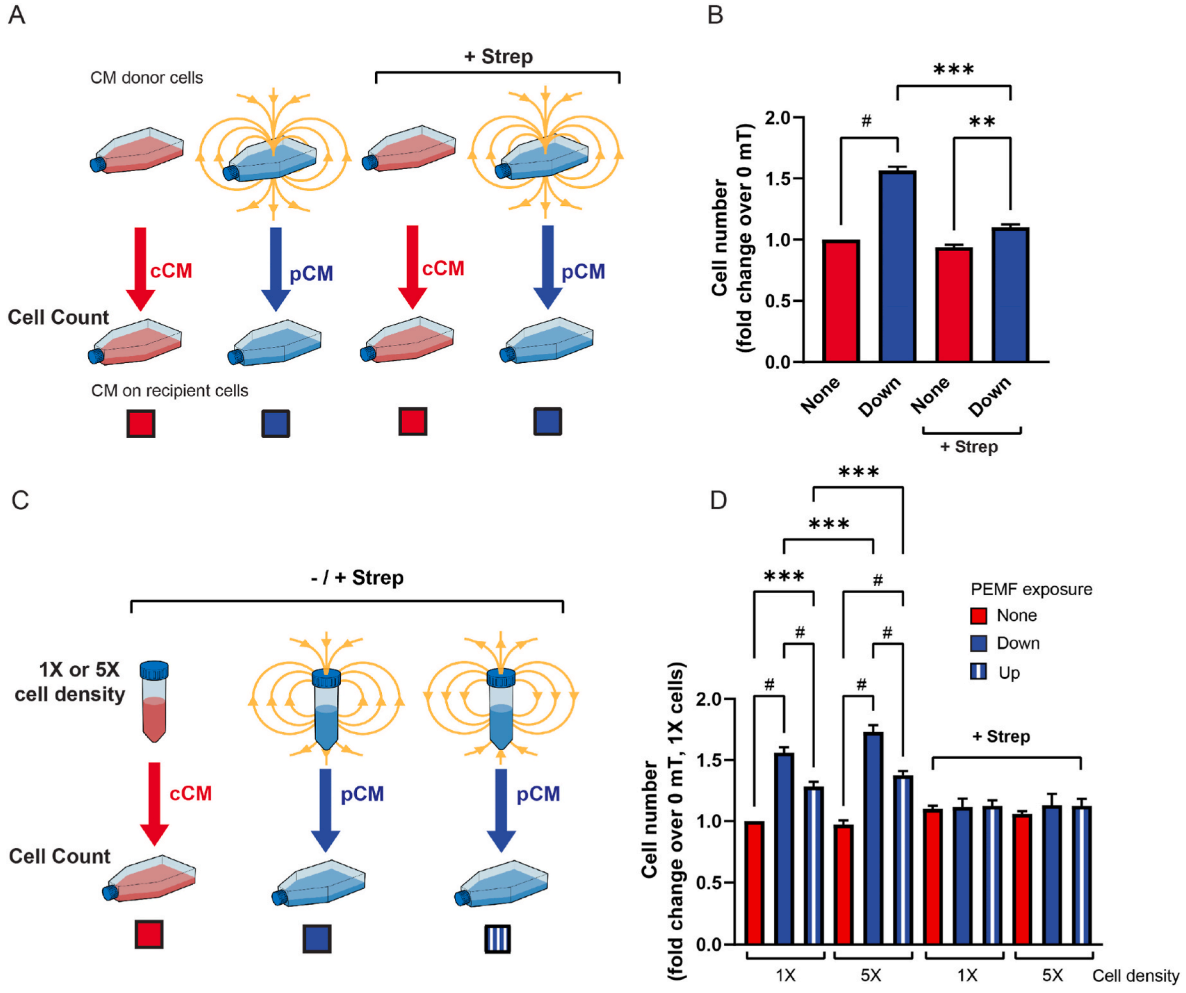

Fig. 3. Aminoglycoside antibiotics block the ability of magnetic fields to stimulate proliferation. A) Depiction of recipient cultures receiving cCM (red) or pCM (blue) that had been generated with or without streptomycin added to the media of the donor cells at the time of downward field exposure (blue) or no exposure (red), as indicated. **B)** Bar chart showing the pooled data for recipient cell numbers expressed as fold change relative to recipient cells in unexposed cCM without streptomycin. Data represents the average of n = 6 biological replicates. **C)** Depiction of recipient cultures receiving cCM (red) or pCM (blue) that had been generated from cells in suspension (either 1X or 5X cell density, with or without streptomycin added) under basal conditions (red) or exposed to downward (solid blue) or upward (vertical blue stripes) magnetic fields. **D)** Bar chart showing the pooled data of induced proliferation from recipient cultures expressed as fold change relative to 1X cultures receiving unexposed cCM without streptomycin. Data represents the average of n = 7–13 biological replicates. All biological replicates were derived from the means of three technical replicates. All magnetic exposures consisted of PEMFs at an amplitude of 1.5 mT applied once for 10 min. Error bars represent the standard error of the mean, with $^{**}p < 0.01$, $^{***}p < 0.001$, and $^{\#}p < 0.0001$ analyzed using One-Way ANOVA with Sidak's multiple comparisons test. "None" refers to cultures given cCM or no magnetic exposure.

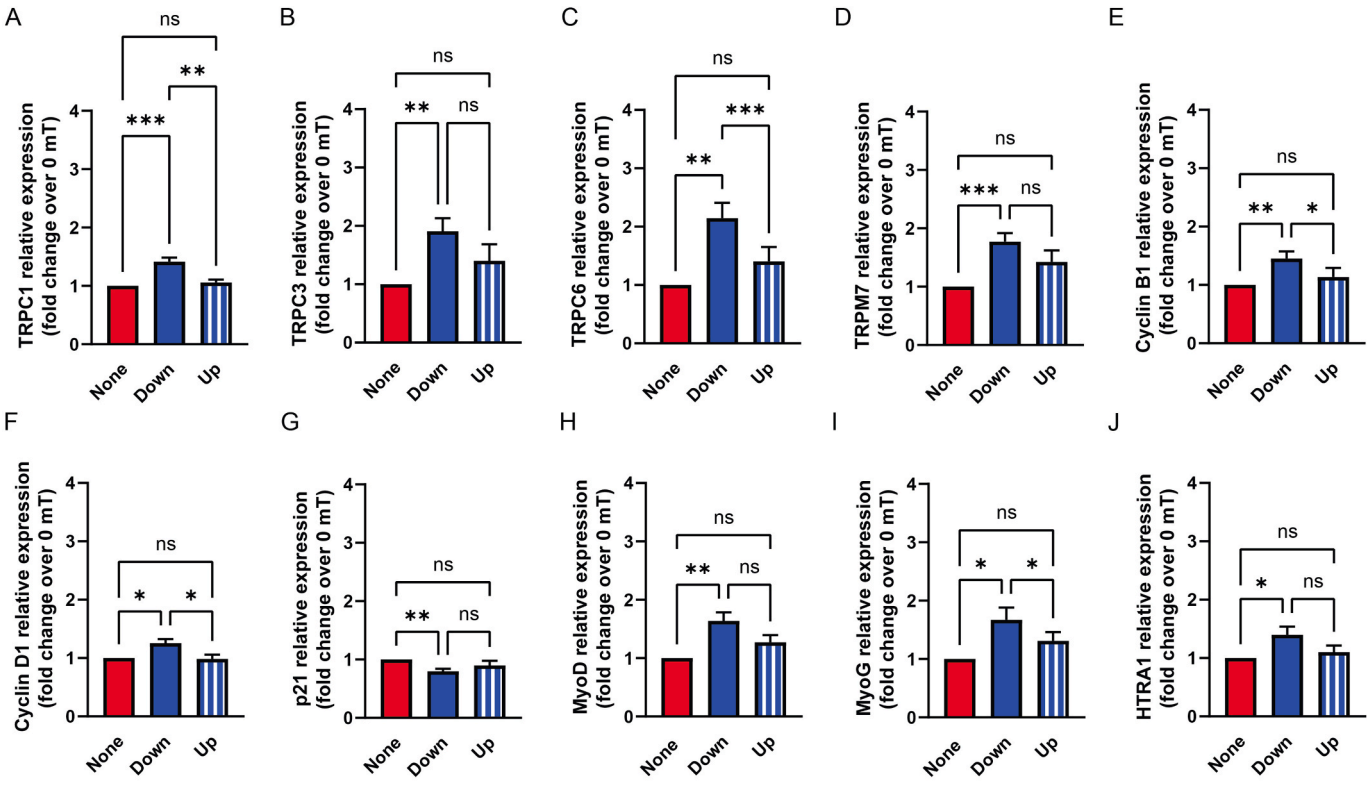

Fig. 4. Direct exposure of myoblasts to downward fields preferentially enhances TRPC channel, cell cycle progression and myogenic regulator protein expressions. Quantification of the relative protein expression (normalized to GAPDH) for **A**) TRPC1, **B**) TRPC3, **C**) TRPC6, **D**) TRPM7, **E**) Cyclin B1, **F**) Cyclin D1, **G**) p21, **H**) MyoD, **I**) MyoG and **J**) HTRA1 from cells directly exposed to downward (solid blue) or upward (vertical blue stripes) magnetic fields expressed as fold change with respect to the unexposed condition (0 mT; solid red). Data represents the average of n = 10–12 biological replicates. All magnetic exposures consisted of PEMFs at an amplitude of 1.5 mT applied once for 10 min. Protein expression was determined 24 h after direct exposure to PEMFs of the indicated characteristics. Error bars represent the standard error of the mean, with $*p < 0.05$, $**p < 0.01$, and $***p < 0.001$, analyzed using One-Way ANOVA with Sidak's multiple comparisons test. "ns" indicates statistical nonsignificant differences. "None" refers to cultures with no magnetic exposure.

Supplementary video related to this article can be found at https://doi.org/10.1016/j.biomaterials.2022.121658

3.6. Direct exposure to PEMFs induces ROS production

Brief (10 min) exposure to 1.5 mT amplitude PEMFs is capable of inducing a low level of reactive oxygen species (ROS) that promote myoblasts into myogenesis [23], whereas longer exposures (1 h) to greater amplitudes (3 mT) PEMFs produces damaging oxidative stress in breast cancer cells [31]. These apparently dichotomous effects are a reflection of the mitohormetic nature of PEMF exposure [23], whereby mild PEMF exposure induces low levels of oxidative stress that are adaptive and enhance survival, whereas stronger PEMF exposure produces greater levels of oxidative stress that are instead overwhelming to a cell's anti-oxidant defenses, stymying their survival [52]. Therefore, despite mitochondrial ROS production being potentially beneficially adaptive, some level of enzymatic disruption may be expected at a cost of requisite oxidative stress. We thus investigated whether ROS production is a feature shared by direct exposure to PEMFs and pCM provision (Fig. 6). ROS levels significantly incremented in myoblasts directly exposed to PEMFs (Fig. 6a–b), but were not apparent in naïve myoblasts provided pCM (Fig. 6d and e). Aligning with previous results, ROS production was greater following downward field exposure (Fig. 6b). Consistent with previously published results demonstrating that a history of cell overgrowth mitigates sensitivity to magnetic field exposure as a result of TRPC1 downregulation [23], the growth of stock cultures for 3 days prior to re-plating for subsequent analysis precluded ROS response to direct magnetic exposure of either direction (Fig. 6c), whereas cells originating from stock cultures grown for only 2 days revealed ROS responses to downward field exposure (Fig. 6b). Furthermore, magnetically-induced ROS production was also smaller from myoblast cultures directly grown at higher density (27%; 6000 cells/well) than at lower density (34%; 3000 cells/well) (Fig. 6b). Analogously, plating donor cultures at a 5-fold higher density than normal (1X) reduced the proliferative potency (%5X-%1X) of the pCM generated by downward or upward exposures by ~ -15% and ~-13%, respectively (Fig. 6f), despite there being a 5-fold greater number of cells contributing to the secretome response. This effect contrasts with the cell suspension scenario, whereby the pCM generated by downward or upward exposures of high-density (5-fold) cell suspensions enhanced the proliferation of recipient cultures by ~+24% and ~+15%, respectively (Fig. 3d). The absence of oxidative stress when pCM is administered alone may underlie its greater myogenic response compared to direct exposure (Fig. 5 versus Fig. 4, respectively). In summary, ROS may not be a necessary evil to benefit from PEMF exposure as associated developmental benefits could be bestowed with secretome administration to unexposed cells or tissues and without the restrictions imposed by contact-inhibition of myoblast responses [53] to magnetic fields [23].

3.7. Effects of pCM on myogenic differentiation and survival

Protein markers of myogenic differentiation were upregulated in myoblast cultures following either direct exposure (Fig. 4) or provision of pCM (Fig. 5) generated in response to downward magnetic fields. Provocatively, the conditioning of base media (DMEM without serum) by myoblasts exposed to downward magnetic fields and then administering to myoblasts in the form of differentiation media (supplemented with 2% Horse Serum) (Fig. 7ai) stimulated myogenic differentiation

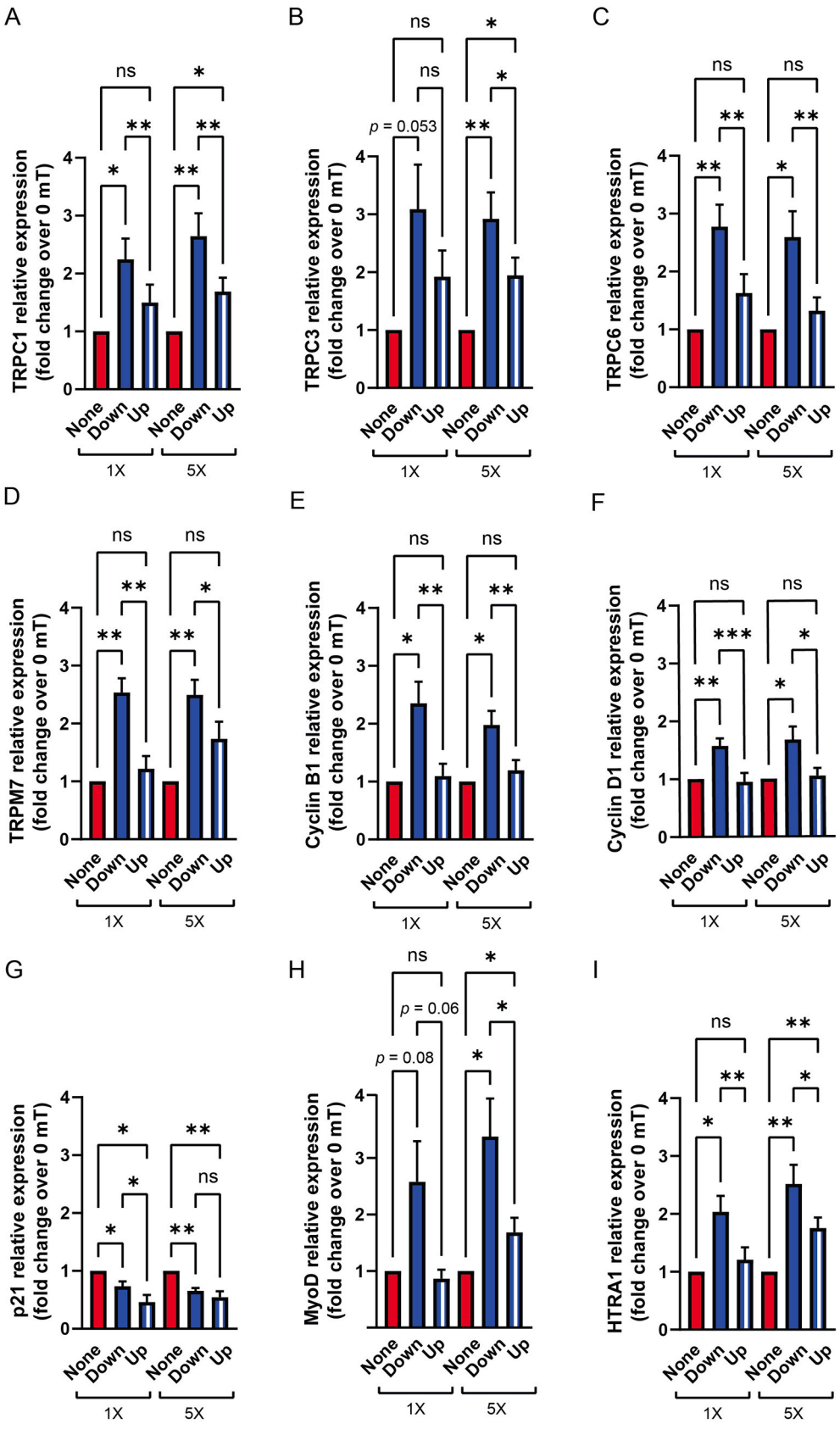

Fig. 5. TRPC channel and myogenic protein expression is more strongly enhanced by pCM delivery. Relative protein expression (normalized to GAPDH) for **A**) TRPC1, **B**) TRPC3, **C**) TRPC6, **D**) TRPM7, **E**) Cyclin B1, **F**) Cyclin D1, **G**) p21, **H**) MyoD and **I**) HTRA1 from cells administered conditioned media harvested from myoblasts exposed to downward (pCM; solid blue) or upward (pCM; vertical blue stripes) magnetic fields expressed as fold change relative to cells given cCM (0 mT; solid red). Data represents the average of n = 5–6 biological replicates. Protein expression was determined 24 h after the provision of the respective conditioned media. All magnetic exposures consisted of PEMFs at an amplitude of 1.5 mT applied once for 10 min. Error bars represent the standard error of the mean, with $^{*}p < 0.05$, $^{**}p < 0.01$, and $^{***}p < 0.001$ or as indicated, analyzed using multiple paired *t*-tests. "ns" indicates statistical nonsignificant differences. "None" refers to cultures given cCM.

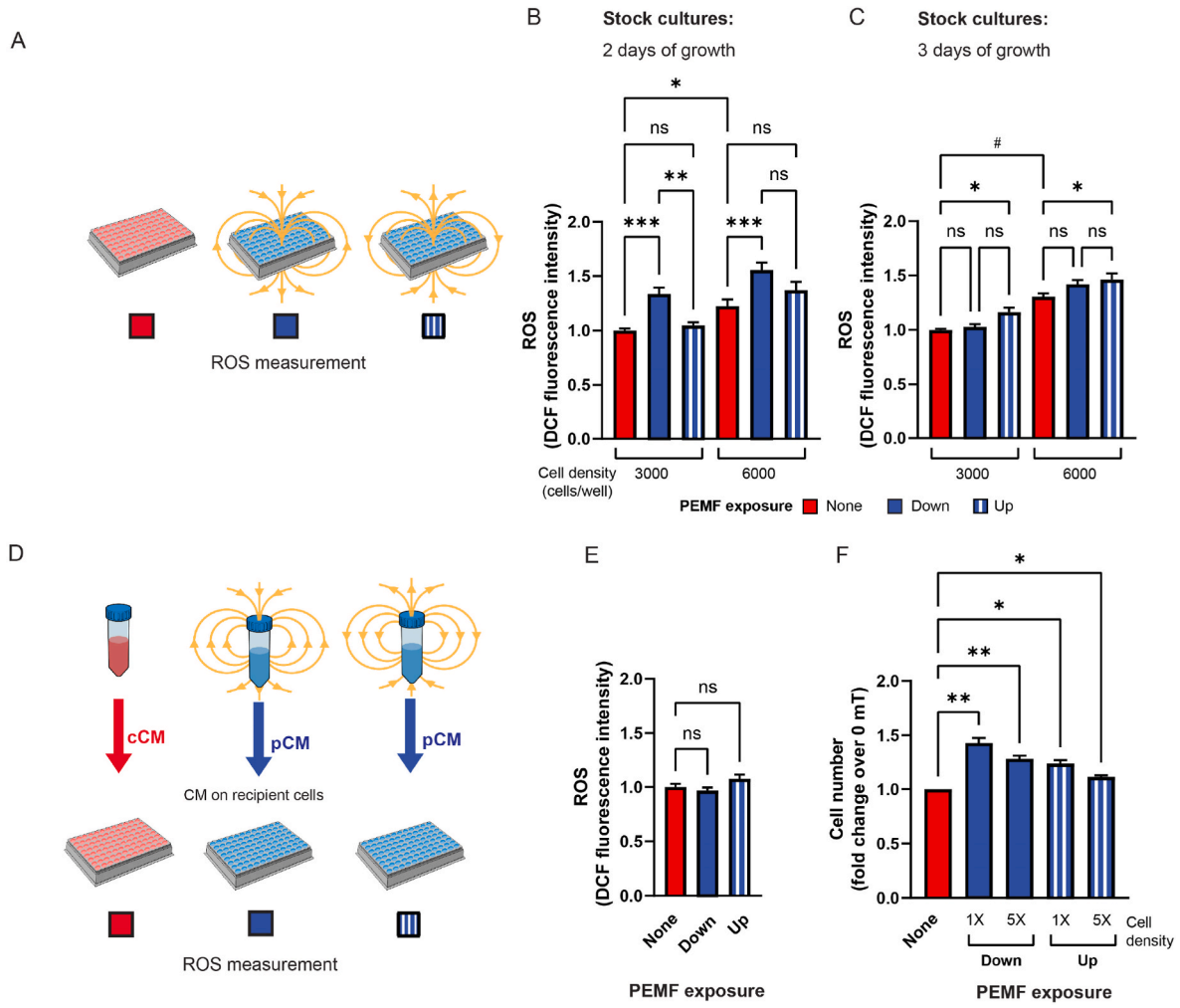

Fig. 6. Direct magnetic exposure creates oxidative stress, whereas secretome delivery does not, and is modulated by cell density. A) ROS production in response to direct PEMF exposure. Myoblasts were seeded at a cell density of 3000 or 6000 cells/well from stock cultures grown for **B**) 2 days or **C**) 3 days. Bar charts show the relative fold change of DCF fluorescence intensity normalized to unexposed 3000 cells/well condition (red bar, left). **D**) ROS production in response to the administration of cCM or pCM delivered to naïve myoblasts in 96-well plates was measured and expressed as the relative DCF fluorescence intensity normalized to cCM **E**), as indicated. ROS measurements were taken 4 h post PEMF exposure. **F**) pCM proliferative capacity is attenuated by high cell density at the time of media collection. Bar chart showing the pooled data for recipient cell numbers expressed as fold change relative to their respective recipient cells (control) in unexposed cCM at 1X or 5X cell densities. Data represent the average of n = 3 biological replicates. Error bars represent the standard error of the mean, with $^{*}p < 0.05$, $^{**}p < 0.01$, $^{***}p < 0.001$ and $^{\#}p < 0.0001$, analyzed using One-Way ANOVA with Sidak's multiple comparison tests. "ns" indicates statistical nonsignificant differences. "None" refers to cultures given cCM or no magnetic exposure.

(myogenin nuclear translocation, iii; desmin protein expression, v) and myotube formation (fusion index, iv), while slowing proliferation (cyclin D1 protein expression, vi), relative to unconditioned DMEM or DMEM conditioned to upwardly directed magnetic fields (Fig. 7aii-vi). Notably, despite a greater number of cells (nuclei) in the culture given cCM (none or 0 mT) nuclear myogenin staining was significantly less (Fig. 7aii). Thus, it appears that conditioned media collected from appropriately magnetically-exposed myoblasts provide secretome components supporting both proliferation (Fig. 5) and differentiation (Fig. 7a), depending on the context of delivery. Conversely, the administration of downward magnetically-conditioned media harvested from differentiated myotubes, promoted the differentiation of proliferating myoblasts and forestalled proliferation (Fig. 7b). This result indicates that the contents and attributes of the muscle magnetically-induced secretome is also stage-specific and should be taken into consideration when designing secretome-collecting paradigms. Finally, myoblast conditioning of basal media (minus serum) to downward fields conferred better survival than basal media supplemented with fetal bovine serum (5%) as indicated by dichotomous effects on phospho-ERK and phospho-JNK [54–56] (Fig. 7c) and alluding to the potency of freshly generated secretome.

3.8. Validation on porcine myoblasts

The thus far presented data was generated using the C2C12 muscle murine cell line. To address questions of translatability, the effects of downward magnetic field exposure were validated in an immortalized porcine myoblast cell line. Porcine myoblasts exhibited the characteristic preferential proliferative enhancement to downward magnetic field exposure (Fig. 8a) as well as to pCM generated from either murine C2C12 (Fig. 8b) and porcine (Fig. 8c) myoblasts in response to downward field exposure, demonstrating cross-species efficacy. EVs are an important component of FBS contributing to its myogenic potential across species [57]. EVs isolated from C2C12 myoblasts were capable of stimulating the proliferation of porcine myoblasts (Fig. 8d) to a similar degree as direct exposure (Fig. 8a) or pCM provision from either C2C12 (Fig. 8b) or porcine (Fig. 8c) myoblasts, indicating they are a major contributor to the observed secretome responses.

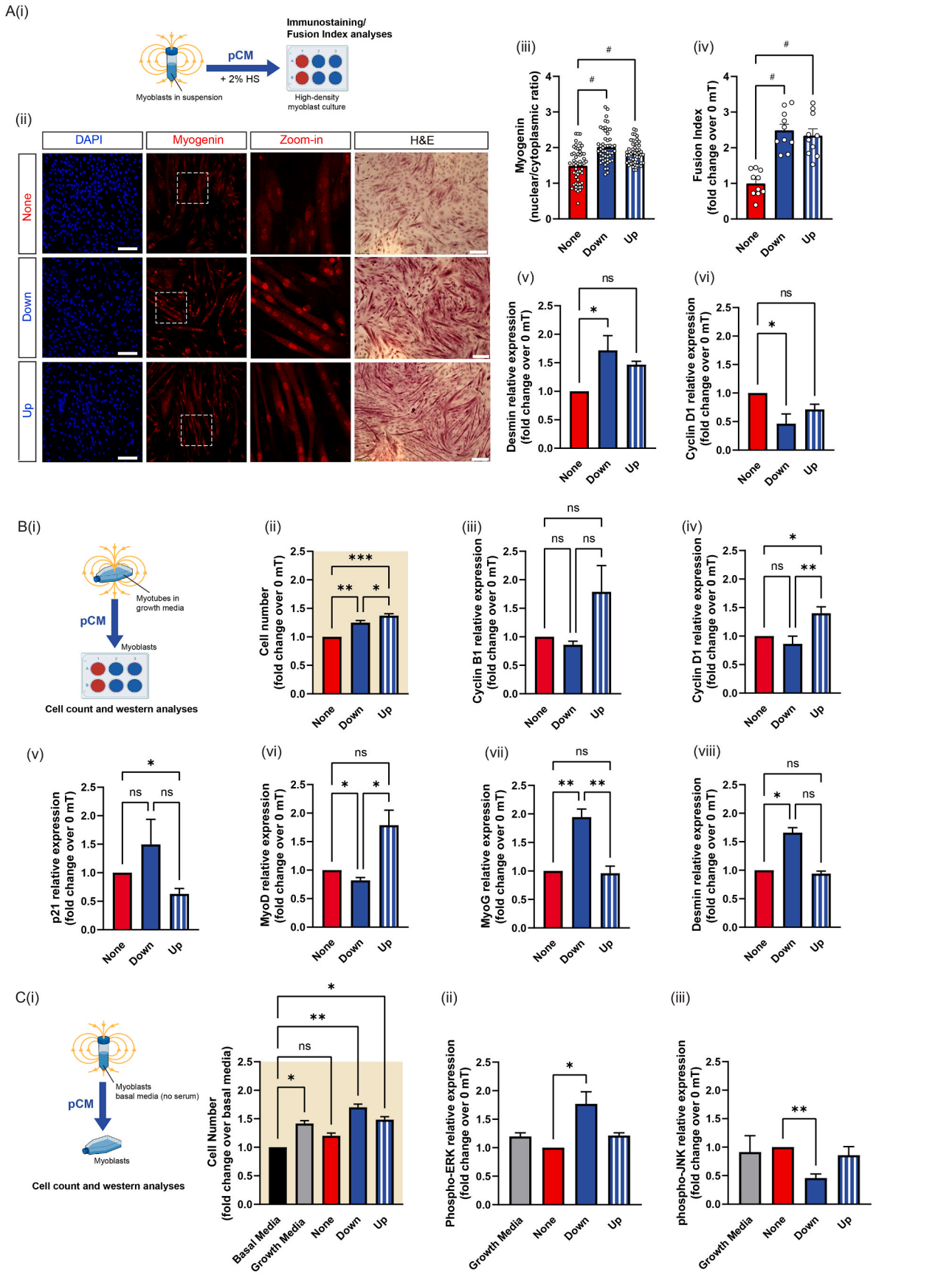

(caption on next page)

Fig. 7. pCM collected from magnetically-stimulated myoblasts and myotubes promote myogenic differentiation and survival. A) (i) Myogenic differentiation in response to myoblast pCM. DMEM was conditioned from exposed/unexposed myoblasts in suspension and then supplemented with 2% HS before administering to pre-seeded day-4 myoblasts. (ii) Confocal images and H&E staining of myotubes 4 days post-pCM administration showing nuclear localization of myogenin and myotube densities. (iii) Ratio of myogenin positive nuclei normalized to cytoplasmic intensity (n=>50 cells/condition). Scale bar = 120 μm. (iv) Myotube fusion index. Scale bar = 100 μm. Relative protein expression of (v) Desmin and (vi) Cyclin D (n = 3 biological replicates). **B)** (i) Myogenic differentiation in response to pCM from myotubes. (ii) Myoblast proliferation in response to myotube pCM. Protein expression of the proliferation markers, (iii) Cyclin B1, (iv) Cyclin D1 , (v) p21 , and differentiation markers, (vi) MyoD , (vii) MyoG and (viii) Desmin, analyzed 24 h post-pCM incubation (n = 6 biological replicates/condition). **C)** Myoblast survival in response to pCM with and without FBS supplementation. (i) Myoblast proliferation in response to basal media (DMEM without FBS), growth media (DMEM plus 5% FBS) or pCM from myoblast in serum-free DMEM (n = 4 biological sets with 3 technical replicates/condition). Relative abundance of phosphorylated (ii) ERK and (iii) JNK normalized to total ERK and total JNK proteins, respectively (n = 3 biological replicates per condition). Error bars represent the standard error of the mean, with $^{*}p < 0.05$, $^{**}p < 0.01$, $^{***}p < 0.001$ and $^{\#}p < 0.0001$, analyzed using One-Way ANOVA with Sidak's multiple comparison tests. "ns" indicates statistical nonsignificant differences. "None" refers to cultures given cCM.

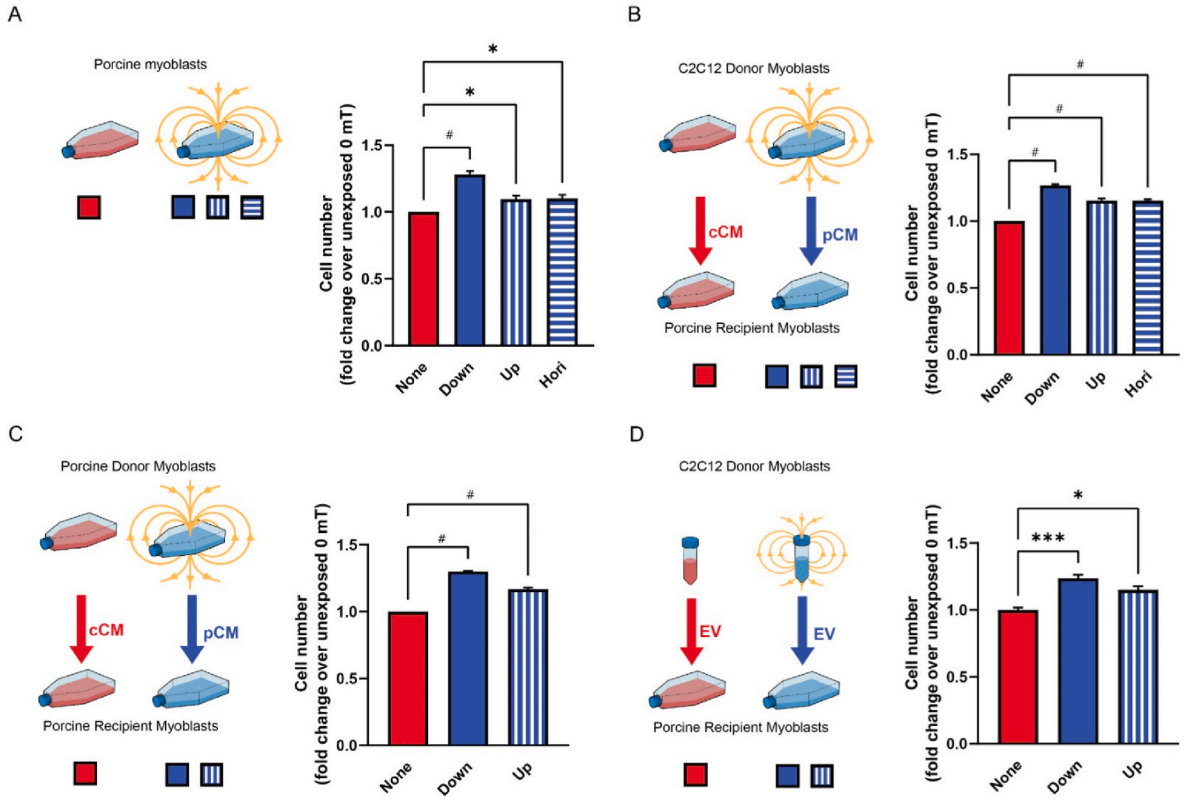

Fig. 8. Porcine myoblast responses to directional magnetic fields and pCM. Different experimental paradigms on porcine myoblasts (schematics). **A)** Porcine myoblasts proliferation in response to no exposure, or direct down, up, or horizontal exposure, as indicated. **B**) Porcine myoblast (recipient) proliferation in response to C2C12 donor pCM or **C**) porcine donor pCM was generated under the different field orientations, as indicated. **D)** Porcine myoblast (recipient) proliferation in response to EVs isolated from C2C12 donor pCM. Cell enumeration was conducted 24 h post magnetic stimulation **A**) or 24 h post pCM or EV administration (**B**, **C** and **D**). All data represent the average of n = 3 to 4 biological replicates with each consisting of 3 technical replicates. Error bars represent the standard error of the mean, with $^{*}p < 0.05$, $^{***}p < 0.001$ and $^{\#}p < 0.0001$, analyzed using One-Way ANOVA with Sidak's multiple comparison tests. "ns" indicates statistical nonsignificant differences. "None" refers to cultures given cCM or no magnetic exposure.

3.9. Secretome characterization

The myogenic potentials of the EV and supernatant fractions of the C2C12 secretome were compared (Fig. 9a). EVs were more capable of promoting proliferation than the supernatant fraction (Fig. 9b), particularly in response to downward-directed magnetic fields (solid blue). Transmission electron microscopic examination of the vesicular fraction revealed spherical bodies on the order of 100–200 nm in diameters (Fig. 9c). Flow cytometry analysis of the EV fraction revealed the presence (per 500,000 events) of characteristic molecular markers of EVs (Fig. 9d), including the tetraspanin, CD9 and CD81 [32]. Despite low levels of detection by flow cytometry, CD9 protein could be detected by Western analysis in the EV fraction, but not supernatant (Fig. 9e). Nanoparticle Tracking Analysis revealed typical particle size distributions in the EV fractions of all three conditioned media scenarios, up, down and no magnetic fields (Fig. 9f). Notably, vesicle diameter tended to increase in the downward field generated sample, whereas particle number tended to decrease in the upward field generated sample (Supplemental Table 1). Multiplex immunoassay of myokine expression from the pCM generated from myoblasts in suspension showed nominal changes in soluble myokine release in response to downward magnetic exposure (Fig. 9g; Supplemental Figure 3), despite a 24-fold concentration of the pCM from that commonly delivered to the cells. The sum of these results indicates that EVs comprise the predominant component of the magnetically-mobilized secretome generated in the suspension cell paradigm after brief periods (≤1 h) of media conditioning.

4. Discussion

The importance of the muscle secretome for physiological

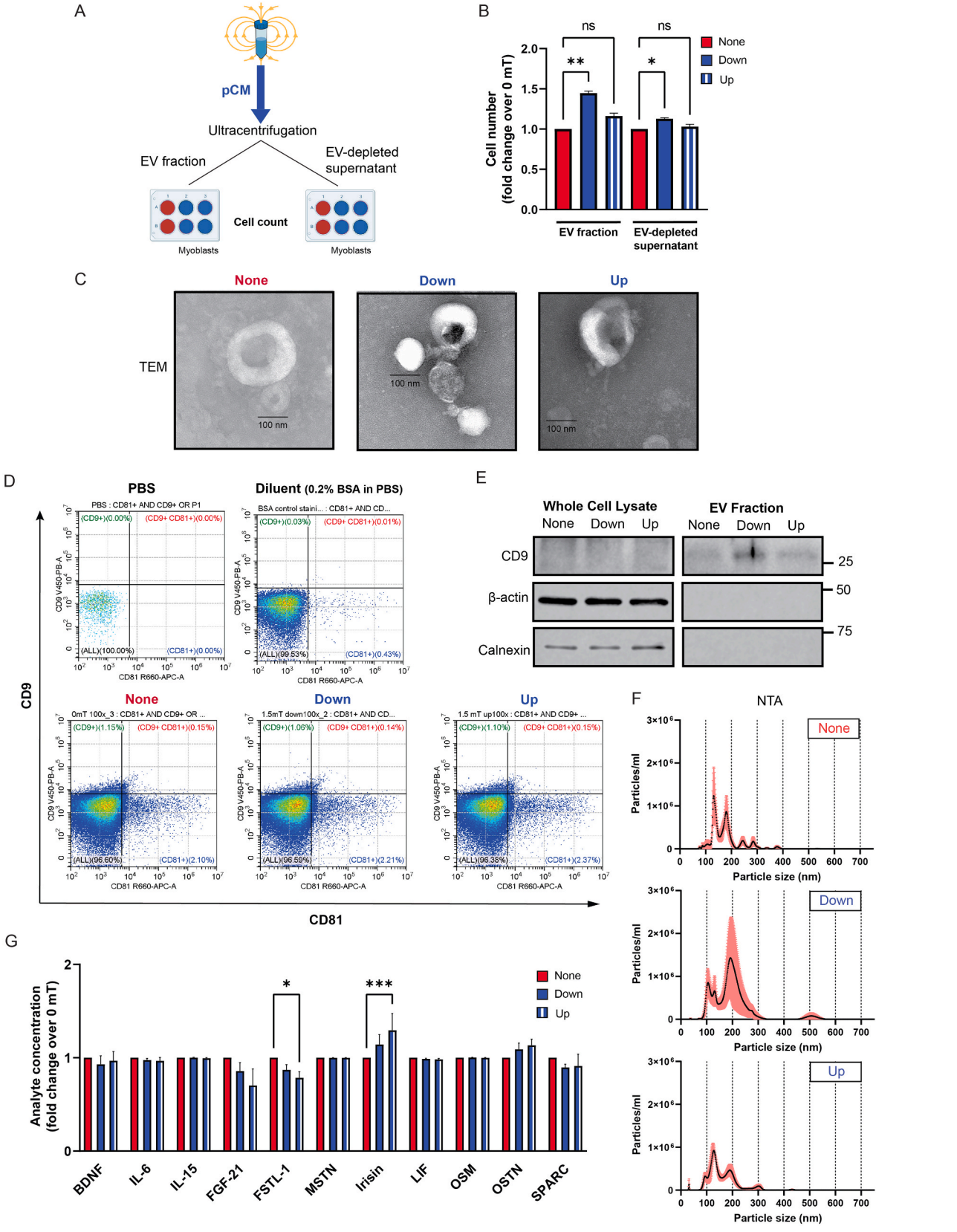

(caption on next page)

Fig. 9. Secretome characterization. A) Schematic depiction of the experimental paradigm used for the generation of EV and EV-depleted pCM to assess the proliferation responses of C2C12 (recipient) myoblasts. C2C12 myoblasts in suspension were exposed to PEMFs and then allowed to condition the media for 1 h (37 °C in the incubator) prior to EV isolation. **B)** Myoblast proliferation assessment 24 h following EV or EV-depleted pCM provision to recipient myoblasts (n = 4 biological replicates with each consisting of 3 technical replicates). **C)** Transmission electron microscopy (TEM) images of EVs isolated from C2C12 cCM and pCM. Scale bar = 100 nm. **D)** Flow cytometric analysis of C2C12 EVs using fluorescent-labeled CD9 and CD81. Detection levels given per 500,000 events. **E)** Representative Western blot images of EV marker, CD9 and cytoskeletal and endoplasmic reticulum markers, actin and calnexin, demonstrating the absence of cellular contamination of the EV preparation. **F)** Representative NTA histogram showing size distribution and abundance of C2C12 EVs. Also see Supplemental Table 1. **G)** Quantitative analysis of cCM and pCM soluble factors using multiplex immunoassay analysis (n = 9 biological replicates each consisting of 3 technical replicates). Error bars represent the standard error of the mean, with $*p < 0.05$, $**p < 0.01$, $***p < 0.001$, analyzed using One-Way ANOVA with Sidak's multiple comparison tests. "ns" indicates statistical nonsignificant differences. "None" refers to cultures given cCM or no magnetic exposure.

homeostasis is broadly accepted [1,2,6]. Muscle is the body's largest secretory tissue and the greatest source of trophic, inflammatory- and disease-regulating factors delivered to the body via the systemic circulation. An increase in mitochondrial respiration initiates transcriptional cascades that ultimately culminate with the activation of the muscle secretome [11], most commonly invoked by physical activity [8,9]. Brief exposure to low-energy magnetic fields holds the capacity to activate mitochondrial respiration [23] as well as recapitulate many of the hallmark metabolic responses associated with exercise in mice [24], raising the intriguing possibility of similar exposure paradigms being exploitable to mobilize the muscle secretome for a myriad of health and commercial applications.

In this study, we extend our previous understanding of *in vitro* magnetic developmental induction by demonstrating best developmental response to downwardly directed magnetic fields in the areas of proliferation, differentiation and survival via the analyses of protein expression, mitochondrial activation (ROS production), secretome composition/responses, videography (Supplemental Videos S1a and S1b; Supplemental Figure 4), as well as arising from diverse devices and species. Notably, the developmental potency of magnetic exposure may have been underestimated in previous studies given that the applied fields were delivered in the upward [28] and horizontal [58] orientations. Moreover, nearly all published studies have also been conducted in the presence of streptomycin that as shown here (Fig. 3) and elsewhere [23,25,26,28,35] to preclude developmental responses to analogous magnetic stimulation. In this report, we largely focused on the myoblast responses for simplicity of execution (exposure 24 h after plating), uniformity of cell status (undifferentiated), ability to conduct directionality experiments in suspension cultures, and ease of analysis (proliferation assessment). Nonetheless, we were capable of demonstrating directionally-specific magnetically-induced myogenic enhancement of myotube secretome despite these noted experimental complexities (Fig. 7a and b). The existence of a technical platform for the effective and prompt mobilization of the muscle secretome using well-defined, safe and non-invasive magnetic fields has broad clinical and commercial applications.

4.1. TRPC-mediated magnetic induction

Biological responses to extremely low-frequency magnetic fields, analogous to those employed in the present study, were previously shown to correlate with TRPC1 expression [23,24,26,31]. TRPC1 and TRPM7 are the two most ubiquitously expressed of all TRP channels, indicating developmental relevance [59]. Basal myoblast proliferation was previously shown to more closely correlate with the expression of TRPC1, than that of TRPM7 [60]. Magnetically-stimulated myogenic proliferation could be abrogated by genetic silencing of TRPC1, but not of TRPM7, as well as correlated most strongly with TRPC1 expression than to other TRP channels [23]. Demonstrating necessity and sufficiency, selective vesicular delivery of TRPC1 was sufficient to reinstate mitochondrial magnetoreception in myoblasts genetically-engineered to be deficient in the said process by TRPC1 knockdown [27]. Magnetic myogenic induction could also be completely blocked with moderately selective pharmacological antagonism of TRPC1 with 2-APB, SKF-96365 or the aminoglycoside antibiotics [23]. The aminoglycoside antibiotic, streptomycin, was utilized as a TRPC1 channel antagonist in the present study to maintain relevancy to existing *in vitro* clinical and commercial applications that conventionally employ its prophylactic use. Nonetheless, the contribution of other TRPC channel classes to magnetoreception cannot be discounted as they are known to heteromultimerize and combine functionalities [50] and will be the subject of future investigations.

4.2. Aminoglycoside antibiotic antagonism of magnetoreception – medical and commercial implications

Reproducibility problems in the field of bioelectromagnetic may have previously arisen due to the widespread use of the aminoglycoside antibiotics during *in vitro* investigations. The aminoglycoside antibiotics have been shown to prevent magnetically-stimulated myogenesis [23] and neurogenesis [26] via their capacity to antagonize TRPC1 function. Here, we show that the transient addition of streptomycin, timed to coincide with PEMF exposure, was also sufficient to prevent the production of a pCM capable of stimulating myoblast proliferation (Fig. 3) that coincided with TRPC1 expression (Fig. 4). TRPC1 is the most ubiquitously expressed of all TRP channels [59], underscoring its developmental importance. TRPC1-mediated mechanotransduction channels have also been shown to be mitigated by the presence of streptomycin in skeletal muscle [61–63] and neurons [64] as well as precluded the consequent increase in mitochondrial respiration [65]. Therefore, the common use of aminoglycoside antibiotics has likely compromised the investigation of TRPC1-transduced developmental processes, potentially leading to erroneous interpretation of some of the findings reported in previous studies. Indeed, magnetism [23] and gravity [36,66] are the two most persistent biophysical ambient forces contributing to basal *in vitro* developmental programs, whose reception has now been linked to TRPC1. Given that magnetic fields and mechanical forces are ever-present and of obvious developmental importance, the extensive use of the aminoglycoside antibiotics has surely confounded the relevancy and interpretation of past and ongoing *in vitro* studies in the areas of human regenerative medicine, agriculture and the synthetic food industry. Finally, these results forewarn against the widespread prophylactic use of the aminoglycoside antibiotics in the general population as an associated antagonism of muscle secretome responses could have global health ramifications.

4.3. Biophysical implications of magnetic field direction specificity

Most studies examining the effects of extremely low-frequency magnetic fields have not taken into consideration magnetic field directionality [29]. One hypothesis for how cells may perceive magnetic fields is via the production of induced ionic currents. Predicted from physical principles, magnetic fields (Supplemental Figure 1, gold arrows) should induce ionic current flow at the membrane surface (Supplemental Figure 1, blue arrows) orthogonal to their plane of entry [34], such that the greatest current induction will be associated with the greatest degree of cross-alignment between the penetrating magnetic field lines and the major plane of cell spreading, independently of the absolute plane of rotation of the greatest cross-alignment. Moreover, via such a scheme, for a given cell orientation, up and down fields should be

perceived identically (Supplemental Figure 1a*ii* and a*iii*; identical length of blue arrows). To this end, flasks were placed in a "standing" (vertical) position and exposed to magnetic fields directed either in the up or down directions (Supplemental Figure 1b). Despite having identical induced current path lengths (blue arrows), downward fields continued to be superior at stimulating proliferation (Supplemental Figure 1c, solid blue), although relatively modest when compared to that observed with horizontally positioned flasks (Figs. 1 and 2a-d, Supplemental Figure 1e; solid blue), where the induced current path is greater (Supplemental Figure 1d*ii*), yet still more responsive to downward fields (Supplemental Figure 1f, solid blue). These results confirm that downward field exposure *per se* exerts a stronger proliferative stimulus, independently of general cell orientation. To further dissociate between the relative contributions of downward and orthogonal magnetic exposures, flasks were placed in a standing orientation and exposed to fields in the horizontal direction (Supplemental Figure 1e, hatched blue), in effect recreating the magnetic field-to-cell flask cross-alignment of Supplemental Figure 1e (solid blue; also see Fig. 2a–d) for the downward exposure of horizontal flasks, but rotated 90° as schematized in Supplemental Figure 1e (hatched blue). Downward fields applied to horizontally positioned flasks continued to provide a greater stimulation for proliferation than did horizontally-directed fields applied to vertical flasks (Supplemental Figure 1f), although both exhibiting identical induced path length (Supplemental Figure 1d*ii* and *iv*), indicating that the predominant deciding factor of magnetic sensitivity is indeed downward field directionality. The relative dominance of downward field exposure was corroborated in cell suspensions (non-oriented) (Figs. 1–3) and in diverse magnetic field devices (Supplemental Figure 2), providing further evidence of the authenticity of the effect. The sum of our results underscores the dominance of downwardly directed magnetic fields in inducing paracrine-mediated developmental responses.

A differential effect of downward versus upward magnetic field exposure has been described with respect to strong static magnetic fields (1 T) applied for a few days [67], albeit in the presence of streptomycin. Under these conditions upward magnetic fields were found to inhibit cancer cell growth in adherent cultures, whereas downward fields produced no statistically significant effect. On the other hand, both downward and upward magnetic fields inhibited the growth of cancer cells in suspension, corroborating that cell-to-cell contact can influence response to magnetic field exposure (Fig. 6). Here, we show that brief (10 min) exposure to low amplitude (1.5 mT) downward pulsing magnetic fields is more potent at inducing proliferation in both adhered and cells in suspension via secretome means. Other factors that may account for the distinct responses of Tian *et al.* [67] from those reported here may be the elevated respiratory capacity of cancer cells and their use of chronic strong static magnetic fields (1000× greater than our time-variant magnetic fields), both of which are mitohormetic determinants [52] that can negatively impact survival when their effects are combined [31].

4.4. Biological magnetic field direction sensitivity

Two principal mechanisms have been proposed to account for the ability of an organism to sense and respond to the orientation and direction of the geomagnetic field, the Ferromagnetite and Radical Pair Mechanisms (RPM) [68,69]. In the ferromagnetite mechanism, magnetic fields are detected by iron oxide (Fe_3O_4) nanocrystals that are tethered to cellular structures and exhibit magnetic remanence. The movement of these ferromagnetite nanocrystals in relation to a magnetic field enables the organism to detect the intensity, inclination and polarity of the magnetic field in the absence of light. On the other hand, the RPM utilizes the quantum physical effects of electromagnetic fields on electron spin dynamics resulting from the photoreduction of flavoenzyme-based reaction centers associated with light-sensitive (blue) cryptochromes (Cry) to detect magnetic field direction and inclination, but not polarity. Magnetic field exposure during photoreduction of flavin moieties precludes the requirement that the delivered energies exceed that of ambient thermal energy (k_BT) in order to induce biological action [68,69], an independence previously demonstrated with the presented magnetic field paradigm whereby shielding myoblasts from all ambient magnetic fields slowed TRPC1-mediated myogenesis [23]. Although typically elicited with field amplitudes on the order of the Earth's geomagnetic field (~50 μT), a radical pair response can also be elicited with low-frequency field exposure in the low milliTesla range such as those employed in the present study [70]. Magnetically-responsive radical pair dynamics have also been shown to induce mitochondrial respiration [71] and ROS formation [71,72], to stimulate proliferation [72], analogously to the fields employed in the present study (Fig. 6) and elsewhere [23]. Recently, a magnetic orientation system has been described in termites that employs both magnetite and radical pair systems to confer both light-insensitive and light-sensitive navigation, respectively [73]. Specifically, Gao *et al.* [73] demonstrated the existence of a comprehensive geomagnetic navigation system requiring the involvement of a magnetite receptor complex, cryptochrome 2 (Cry2) and an odorant-responsive calcium channel, named olfactory co-receptor (Orco) [74–76].

Provocatively, Cry2 has been described in muscle where it is involved in cell cycle progression (cyclin D1) and downstream muscle differentiation [77] in association with mitochondrial regulatory pathways [78], features shared with our magnetic field paradigm in muscle demonstrated here and elsewhere [23,24,27]. Moreover, evidence of a store-operated calcium entry (SOCE) and flavin-dependent, redox-sensitive, photomechanical transduction process requiring the participation of Cry2 and promoting striated muscle development has recently emerged [79]. TRPC channels are the integrators of diverse forms of biophysical stimuli and hence serve as the sensory receptors of the cell [50], a role they subserve by combining their distinct modes of activation via a process of heteromultimerization. Notably, mechanotransduction [36,50,66], magnetotransduction [23,25–27], phototransduction [80–82], SOCE [38] and redox-sensing [65] are parallel activation modes of TRPC1 that would fit the integrative requirement for the implicated calcium extracellular entry and intracellular release pathway for photomechanical transduction. Notably, the TRPC subfamily holds the highest degree of homology to the original *Drosophila* phototransductive TRP channel, founding member of the entire superfamily [50,83]. Moreover, TRPC1 has been directly implicated in phototransduction in diverse species and tissues [80–82], is the most ubiquitously expressed of all TRP channels in mammals [59] and both magnetoreception [23] and photomechanical transduction [79] can be antagonized by the TRPC channel blocker, 2-APB, or other forms of inhibiting extracellular calcium entry, drawing provocative parallels. However hypothetical at present, it is intriguing to speculate that TRPC1 may comprise part of a magnetic signaling complex (analogous to the Orco olfactory sensory receptor channel) conferring directional developmental responses in collaboration with Cry2 and potentially other molecular partners and warrants future experimental exploration, particularly with reference to how downward fields are selectively perceived by the cell.

4.5. Illustrative application: cultivated meat production

A major challenge in cell-based meat production is the development of a method of mass-producing culture medium that is myogenic, cost-effective and safe. Traditionally, this objective has been met through supplementation with exogenous growth factors commonly harvested from the fetuses of livestock [21,22]. Other than being an expensive process, yielding low levels of bioactive factors, this approach also invokes ethical issues surrounding animal cruelty as well as incurs a negative environmental impact. The unmet need was hence a manner to effectively stimulate growth factor release during *in vitro* meat cultivation with minimal intervention.

Mitochondrial respiration triggers enzymatic cascades that

ultimately mobilize secretome release [8–12]. This important contribution of mitochondrial respiration has been largely ignored in conventional cultured meat paradigms, effectively limiting the quality and quantity of the biomass produced. The PEMF platform presented in this study is non-invasive, low-energy, and drug/gene modification-free and is capable of enhancing mitochondrial respiration, myokine release, and myogenesis [23]. A single 10 min exposure of donor muscle cells to correctly oriented PEMFs produces a pCM that after only 30 min of conditioning is capable of enhancing the basal growth of naïve recipient cells by ~50%, demonstrating the adequacy and potency of the magnetically-induced muscle secretome to promote myogenesis. Indeed, pCM was better able to promote the growth and survival of myoblasts than fetal bovine serum (Fig. 7c). Therefore, in an industrial setting, pCM provision may prove more commercially viable than direct magnetic exposure in enhancing cell-based meat production (compare Fig. 4 (direct exposure) and Fig. 5 (pCM provision)), given the demonstrated low level of oxidative stress associated with direct exposure (Fig. 6).

Cell-to-cell contact inhibition [53] places restrictions on secretome efficacy (Fig. 6), that would not exist for cells in suspension (Fig. 3c). The rapid and nearly complete release of the muscle cell secretome from cells in suspension also has the potential to optimize operational costs. We show here that 30 min of media conditioning from cells in suspension is sufficient to produce a pCM (Fig. 3c and d) of similar proliferative capacity as pCM harvested from adherent cells after 6 h of exposure (Figs. 1b, 2d and 3b). Moreover, replacement of the pCM from cells 1 h after exposure with age-matched naïve conditioned media precluded a proliferative response (Fig. 1c), indicating that nearly all of the complete allotment of secretome had been released into the bathing media within an hour of PEMF exposure. Finally, conditioning the media for too long, as to allow cell overgrowth, will produce a secretome with reduced proliferative capacity (Fig. 6f). Magnetic exposure platforms addressing these caveats can be feasibly implemented into existing cell-based meat production pathways with minimal disruption of ongoing production processes, independent of species or ultimate meat objective, and offers key advantages over the state of the art. First, its immediate and highly controllable stimulation of secretome activation from muscle cells will allow for the discovery of secretome components that best support myogenesis. Secondly, it will allow for the scalable production of the secretome from muscle cells in suspension culture, which gains importance in light of our results showing that cell-to-cell contact may potentially undermine the production of a proliferative secretome (Fig. 6f).

Mechanical stimulation is another manner to stimulate myokine release, but is difficult to achieve in conventional bioreactor paradigms with high acuity and uniformity to all cells. The application of mechanical forces to cells in suspension cultures is lossy and dissipative as freely floating cells largely travel with the flow of the fluid with a minimum of substrate-mediated counterforces that are necessary to produce the shear stresses necessary to instigate secretome release. By contrast, magnetic activation stimulates muscle cells in suspension uniformly and with high temporal acuity and secretome release appears to be very efficient. Moreover, such a magnetic approach would also be clean, humane and commandeer the innate ability of muscles to support their own development with the production of essential growth factors. The ultimate objective would be to reduce the need for exogenous supplementation with animal serum or purified myokines (Fig. 7c) as well as drugs, antibiotics, or genetic modification.

4.6. Magnetically-induced secretome

The results generated from myoblasts in suspension upon conditioning the media for 30 min post-PEMF exposure indicate a predominant contribution of EVs in promoting *in vitro* myogenesis in this paradigm (Fig. 9). Although an important contribution of EVs from C2C12 myoblasts [57,84] and fetal bovine serum [57,84] for the execution of myogenesis has been shown, their role in the cultivated meat industry has not been commonly discussed in the scientific literature [19]. The provision of EVs to developing tissues offers practical advantages over the delivery of soluble factors, foremost: **1**) their capacity to be conveniently concentrated for storage and delivery as well as; **2**) potentially loadable with magnetic exposure. The loading of therapeutic compounds into EVs for drug delivery has proven challenging [85]. The data presented in this report would support the notion that appropriately directed magnetic fields may represent a novel and efficient method to load EVs with endogenous therapeutic molecules; EV numbers did not change appreciably upon magnetic exposure, but vesicle size and developmental potency do (Fig. 9f; Supplemental Table 1). The purpose of the present report was to define a technical strategy with demonstrated developmental efficacy. A detailed analysis of the EV contents following magnetic stimulation will be the topic of future investigations. It is also likely that a longer conditioning time would have revealed an important contribution from myokines.

5. Conclusions and outlook

We show that the muscle cell secretome can be effectively activated by brief exposure to pulsing magnetic fields of defined directionality. Given the acknowledged signaling, metabolic and regenerative importance of the muscle secretome, the development of a method to rapidly and non-invasively activate its release without the use of drugs or genetic modification has clear scientific, medical and commercial value. In particular, *in vitro* cell growth commonly requires trophic factor supplementation, either in the form of animal serum or defined factors. We show here that muscle pCM has comparable growth and survival capabilities as conventionally employed fetal bovine serum, which merits pursuing in future investigations.

The main objective of this report was to delineate the fundamental operational requirements for the production of a myogenically favorable magnetically-induced secretome from isolated muscle cells. This technology offers a viable and robust platform for cytokine discovery. Future studies will examine the potential of analogous magnetic stimulation to modulate the secretome responses of differentiated tissues and in behaving animals and will allow for the identification of secretome components that are tissue-, developmental stage- and condition-specific. As cell overgrowth was shown to influence the myoblast secretome response, the presented platform may also provide a discovery platform with which to identify senescence secretome constituents of relevance to muscle and other clinically important tissues. The presented results will also dictate that magnetic field directionality must be taken into consideration when designing future coil systems for *in vivo* (animal or human) or *in vitro* use. Finally, this platform can be ultimately applied to a broad range of other progenitor cell classes of relevance to diverse developmental, clinical and industrial applications.

Funding

This work was largely supported by a charitable donation by the Lee Kong Chian MedTech Initiative, Singapore (N-176-000-045-001) and funding from the Institute for Health Innovation & Technology, iHealthtech, at the National University of Singapore. This EV work was supported by the NUS Yong Loo Lin School of Medicine Nanomedicine Translational Research Program (NUHSRO/2021/034/TRP/09/Nanomedicine) and the NUS NanoNASH Program (NUHSRO/2020/002/NanoNash/LOA) to JWW. SZ would like to acknowledge the Ministry of Education for providing research scholarship to support their graduate study in the Yong Loo Lin School of Medicine, National University of Singapore. MK would like to acknowledge the funding from the Healthy Longevity Translational Research Programme and the Ministry of Education for providing a postdoctoral fellowship at the Yong Loo Lin School of Medicine, National University of Singapore (NUSMED/2020/PDF/05). The publication cost of this article is funded by Lee Kong Chian

MedTech Initiative, Singapore.

Author contributions

AFO and YKT conceived and designed this study. CJKW, YKT, JLYY, CHHF, LSWL, MK and ST performed experiments for the study. CJKW, YKT, JLYY, LSWL, MK, AJF, JWW and AFO analyzed the data. JF provided the initial designs and simulations for the coils systems used in this study. JZL adapted the magnetic field devices employed in this to study changes in field polarity. Fabrication of coil system 2 (animal coil), coil systems 3 and 5 (human leg coil and human breast coil) and coil system 4 (human arm coil) was conducted by Fields at Work GmbH (Zürich, Switzerland), FLEX LTD. (Singapore) and HOPE Technik PTE. LTD. (Singapore), respectively. YKT and AFO wrote the manuscript and all authors approved the final manuscript.

Data availability

The original contributions presented in the study are included in the article. Further inquiries can be directed to the corresponding authors.

Declaration of competing interest

The authors declare the following financial interests/personal relationships which may be considered as potential competing interests: Alfredo Franco-Obregon reports financial support was provided by Lee Foundation. Alfredo Franco-Obregon reports a relationship with QuantumTx Pte Ltd that includes: non-financial support. AFO and JF are inventors on patent WO 2019/17863 A1, System, and Method for Applying Pulsed Electromagnetic Fields as well as a contributor to QuantumTx Pte. Ltd., which elaborates on electromagnetic field devices for human use licensed to National University of Singapore. JZL is currently an employee of QuantumTx Pte. Ltd, and provided technical support for one of the devices in the study. All other authors declare no conflicts of interest.

Acknowledgments

The authors would like to acknowledge Zac Goh (Scientific Illustrator) and Kee Chua Toh (Communications Manager) of the iHealthtech, National University of Singapore for the graphical design and photographic images of the PEMF devices respectively. Larry Sai Weng Loo is funded by Singapore-New Zealand Bilateral Programme on Future Food Grant no. A20D3b0073 by Biomedical Research Council (BMRC), Agency for Science, Technology and Research (A*STAR). We would also like to appreciate the efforts of Tiffany Gan Rui Xuan, Poh Loong Soong, Yi Sheen Chia, Andy Jack Siong Tan, Lih Ting Ching for their earlier exploratory work that unfortunately did not appear in this manuscript. We also like to thank the members of the Biolonic Currents Electromagnetic Pulsing Systems (BICEPS) Laboratory, without which this research would not be possible.

Appendix A. Supplementary data

Supplementary data to this article can be found online at https://doi.org/10.1016/j.biomaterials.2022.121658.

References

[1] K. Karstoft, B.K. Pedersen, Skeletal muscle as a gene regulatory endocrine organ, Curr. Opin. Clin. Nutr. Metab. Care 19 (2016) 270–275.
[2] M.C.K. Severinsen, B.K. Pedersen, Muscle-Organ crosstalk: the emerging roles of myokines, Endocr. Rev. 41 (2020) 594–609.
[3] W. Aoi, Y. Tanimura, Roles of skeletal muscle-derived exosomes in organ metabolic and immunological communication, Front. Endocrinol. 12 (2021).
[4] W. Qin, S.L. Dallas, Exosomes and extracellular RNA in muscle and bone aging and crosstalk, Curr. Osteoporos. Rep. 17 (2019) 548–559.
[5] I.J. Vechetti Jr., B.D. Peck, Y. Wen, R.G. Walton, T.R. Valentino, A.P. Alimov, C. M. Dungan, D.W. Van Pelt, F. von Walden, B. Alkner, Mechanical overload-induced muscle-derived extracellular vesicles promote adipose tissue lipolysis, Faseb. J. 35 (2021), e21644.
[6] B.K. Pedersen, M.A. Febbraio, Muscle as an endocrine organ: focus on muscle-derived interleukin-6, Physiol. Rev. 88 (2008) 1379–1406.
[7] M. Sellami, N.L. Bragazzi, B. Aboghaba, M.A. Elrayess, The impact of acute and chronic exercise on immunoglobulins and cytokines in elderly: insights from a critical review of the literature, Front. Immunol. 12 (2021), 631873.
[8] J. Li, Y. Li, M.M. Atakan, J. Kuang, Y. Hu, D.J. Bishop, X. Yan, The molecular adaptive responses of skeletal muscle to high-intensity exercise/training and hypoxia, Antioxidants 9 (2020).
[9] R.A. Louzada, J. Bouviere, L.P. Matta, J.P. Werneck-de-Castro, C. Dupuy, D. P. Carvalho, R.S. Fortunato, Redox signaling in widespread health benefits of exercise, Antioxidants Redox Signal. 33 (11) (2020).
[10] M. Ost, V. Coleman, J. Kasch, S. Klaus, Regulation of myokine expression: role of exercise and cellular stress, Free Radic. Biol. Med. 98 (2016) 78–89.
[11] C. Scheele, S. Nielsen, B.K. Pedersen, ROS and myokines promote muscle adaptation to exercise, Trends Endocrinol. Metabol. 20 (2009) 95–99.
[12] Y. Hao, H. Song, Z. Zhou, X. Chen, H. Li, Y. Zhang, J. Wang, X. Ren, X. Wang, Promotion or inhibition of extracellular vesicle release: emerging therapeutic opportunities, J. Contr. Release 340 (2021) 136–148.
[13] G. Li, L. Zhang, D. Wang, L. AlQudsy, J.X. Jiang, H. Xu, P. Shang, Muscle-bone crosstalk and potential therapies for sarco-osteoporosis, J. Cell. Biochem. 120 (2019) 14262–14273.
[14] N.A. Duggal, G. Niemiro, S.D.R. Harridge, R.J. Simpson, J.M. Lord, Can physical activity ameliorate immunosenescence and thereby reduce age-related multi-morbidity? Nat. Rev. Immunol. 19 (2019) 563–572.
[15] C. Fiuza-Luces, A. Santos-Lozano, M. Joyner, P. Carrera-Bastos, O. Picazo, J. L. Zugaza, M. Izquierdo, L.M. Ruilope, A. Lucia, Exercise benefits in cardiovascular disease: beyond attenuation of traditional risk factors, Nat. Rev. Cardiol. 15 (2018) 731–743.
[16] A. Guo, K. Li, Q. Xiao, Sarcopenic obesity: myokines as potential diagnostic biomarkers and therapeutic targets? Exp. Gerontol. 139 (2020), 111022.
[17] A.W. Kow, Prehabilitation and its role in geriatric Surgery, Ann. Acad. Med. Singapore 48 (2019) 386–392.
[18] J.H. Kwon, K.M. Moon, K.W. Min, Exercise-induced myokines can explain the importance of physical activity in the elderly: an overview, Healthcare 8 (2020).
[19] S. Shaikh, E. Lee, K. Ahmad, S.-S. Ahmad, H. Chun, J. Lim, Y. Lee, I. Choi, Cell types used for cultured meat production and the importance of myokines, Foods 10 (2021) 2318.
[20] N.W. Smith, A.J. Fletcher, J.P. Hill, W.C. McNabb, Modeling the contribution of meat to global nutrient availability, Front. Nutr. 73 (2022).
[21] S.Y. Lee, H.J. Kang, D.Y. Lee, J.H. Kang, S. Ramani, S. Park, S.J. Hur, Principal protocols for the processing of cultured meat, J. Anim. Sci. Technol. 63 (2021) 673–680.
[22] R.D. Warner, Review: analysis of the process and drivers for cellular meat production, Animal 13 (2019) 3041–3058.
[23] J.L.Y. Yap, Y.K. Tai, J. Fröhlich, C.H.H. Fong, J.N. Yin, Z.L. Foo, S. Ramanan, C. Beyer, S.J. Toh, M. Casarosa, N. Bharathy, M.P. Kala, M. Egli, R. Taneja, C. N. Lee, A. Franco-Obregón, Ambient and supplemental magnetic fields promote myogenesis via a TRPC1-mitochondrial axis: evidence of a magnetic mitohormetic mechanism, Faseb. J. 33 (2019) 12853–12872.
[24] Y.K. Tai, C. Ng, K. Purnamawati, J.L.Y. Yap, J.N. Yin, C. Wong, B.K. Patel, P. L. Soong, P. Pelczar, J. Fröhlich, C. Beyer, C.H.H. Fong, S. Ramanan, M. Casarosa, C.P. Cerrato, Z.L. Foo, R.M. Pannir Selvan, E. Grishina, U. Degirmenci, S.J. Toh, P. J. Richards, A. Mirsaidi, K. Wuertz-Kozak, S.Y. Chong, S.J. Ferguson, A. Aguzzi, M. Monici, L. Sun, C.L. Drum, J.W. Wang, A. Franco-Obregón, Magnetic fields modulate metabolism and gut microbiome in correlation with Pgc-1α expression: follow-up to an in vitro magnetic mitohormetic study, Faseb. J. 34 (2020) 11143–11167.
[25] D. Parate, A. Franco-Obregón, J. Fröhlich, C. Beyer, A.A. Abbas, T. Kamarul, J.H. P. Hui, Z. Yang, Enhancement of mesenchymal stem cell chondrogenesis with short-term low intensity pulsed electromagnetic fields, Sci. Rep. 7 (2017) 9421.
[26] T.T. Madanagopal, Y.K. Tai, S.H. Lim, C.H. Fong, T. Cao, V. Rosa, A. Franco-Obregón, Pulsed electromagnetic fields synergize with graphene to enhance dental pulp stem cell-derived neurogenesis by selectively targeting TRPC1 channels, Eur. Cell. Mater. 41 (2021) 216–232.
[27] F. Kurth, Y.K. Tai, D. Parate, M. van Oostrum, Y.R.F. Schmid, S.J. Toh, J.L.Y. Yap, B. Wollscheid, A. Othman, P.S. Dittrich, A. Franco-Obregón, Cell-derived vesicles as TRPC1 channel delivery systems for the recovery of cellular respiratory and proliferative capacities, Adv. Biosyst. 4 (2020), e2000146.
[28] D. Parate, N.D. Kadir, C. Celik, E.H. Lee, J.H.P. Hui, A. Franco-Obregón, Z. Yang, Pulsed electromagnetic fields potentiate the paracrine function of mesenchymal stem cells for cartilage regeneration, Stem Cell Res. Ther. 11 (2020) 46.
[29] M. Mansourian, A. Shanei, Evaluation of pulsed electromagnetic field effects: a systematic review and meta-analysis on highlights of two decades of research in vitro studies, BioMed Res. Int. 2021 (2021), 6647497.
[30] S. Crocetti, C. Beyer, G. Schade, M. Egli, J. Fröhlich, A. Franco-Obregón, Low intensity and frequency pulsed electromagnetic fields selectively impair breast cancer cell viability, PLoS One 8 (2013), e72944.
[31] Y.K. Tai, K.K.W. Chan, C.H.H. Fong, S. Ramanan, J.L.Y. Yap, J.N. Yin, Y.S. Yip, W. R. Tan, A.P.F. Koh, N.S. Tan, C.W. Chan, R.Y.J. Huang, J.Z. Li, J. Fröhlich, A. Franco-Obregón, Modulated TRPC1 expression predicts sensitivity of breast cancer to doxorubicin and magnetic field therapy: segue towards a precision medicine approach, Front. Oncol. 11 (2021), 783803.

[32] L. Tong, H. Hao, Z. Zhang, Y. Lv, X. Liang, Q. Liu, T. Liu, P. Gong, L. Zhang, F. Cao, G. Pastorin, C.N. Lee, X. Chen, J.W. Wang, H. Yi, Milk-derived extracellular vesicles alleviate ulcerative colitis by regulating the gut immunity and reshaping the gut microbiota, Theranostics 11 (2021) 8570–8586.
[33] I. Dasgupta, D. McCollum, Control of cellular responses to mechanical cues through YAP/TAZ regulation, J. Biol. Chem. 294 (2019) 17693–17706.
[34] C. Polk, Physical mechanisms by which low-frequency magnetic fields can affect the distribution of counterions on cylindrical biological cell surfaces, J. Biol. Phys. 14 (1986) 3–8.
[35] C. Celik, A. Franco-Obregón, E.H. Lee, J.H. Hui, Z. Yang, Directionalities of magnetic fields and topographic scaffolds synergise to enhance MSC chondrogenesis, Acta Biomater. 119 (2021) 169–183.
[36] T. Benavides Damm, A. Franco-Obregón, M. Egli, Gravitational force modulates G2/M phase exit in mechanically unloaded myoblasts, Cell Cycle 12 (2013) 3001–3012.
[37] S.F. Mansilla, M.B. de la Vega, N.L. Calzetta, S.O. Siri, V. Gottifredi, CDK-independent and PCNA-dependent functions of p21 in DNA replication, Genes 11 (2020).
[38] A.S. Armand, M. Bourajjaj, S. Martínez-Martínez, H. el Azzouzi, P.A. da Costa Martins, P. Hatzis, T. Seidler, J.M. Redondo, L.J. De Windt, Cooperative synergy between NFAT and MyoD regulates myogenin expression and myogenesis, J. Biol. Chem. 283 (2008) 29004–29010.
[39] M. Chen, S. Yang, Y. Wu, Z. Zhao, X. Zhai, D. Dong, High temperature requirement A1 in cancer: biomarker and therapeutic target, Cancer Cell Int. 21 (2021) 513.
[40] Z.G. Lu, A. May, B. Dinh, V. Lin, F. Su, C. Tran, H. Adivikolanu, R. Ehlen, B. Che, Z. H. Wang, D.H. Shaw, S. Borooah, P.X. Shaw, The interplay of oxidative stress and ARMS2-HTRA1 genetic risk in neovascular AMD, Vess. Plus 5 (2021).
[41] J. Chien, G. Aletti, A. Baldi, V. Catalano, P. Muretto, G.L. Keeney, K.R. Kalli, J. Staub, M. Ehrmann, W.A. Cliby, Y.K. Lee, K.C. Bible, L.C. Hartmann, S. H. Kaufmann, V. Shridhar, Serine protease HtrA1 modulates chemotherapy-induced cytotoxicity, J. Clin. Invest. 116 (2006) 1994–2004.
[42] M.A. Folgueira, D.M. Carraro, H. Brentani, D.F. Patrão, E.M. Barbosa, M.M. Netto, J.R. Caldeira, M.L. Katayama, F.A. Soares, C.T. Oliveira, L.F. Reis, J.H. Kaiano, L. P. Camargo, R.Z. Vêncio, I.M. Snitcovsky, F.B. Makdissi, P.J. e Silva, J.C. Góes, M. M. Brentani, Gene expression profile associated with response to doxorubicin-based therapy in breast cancer, Clin. Cancer Res. 11 (2005) 7434–7443.
[43] X. He, A. Khurana, J.L. Maguire, J. Chien, V. Shridhar, HtrA1 sensitizes ovarian cancer cells to cisplatin-induced cytotoxicity by targeting XIAP for degradation, Int. J. Cancer 130 (2012) 1029–1035.
[44] Z. Xiong, Z. Fu, J. Shi, X. Jiang, H. Wan, HtrA1 down-regulation induces cisplatin resistance in colon cancer by increasing XIAP and activating PI3K/akt pathway, Ann. Clin. Lab. Sci. 47 (2017) 264–270.
[45] M.L. Bay, B.K. Pedersen, Muscle-Organ crosstalk: focus on immunometabolism, Front. Physiol. 11 (2020), 567881.
[46] J.S. Kim, D.A. Galvão, R.U. Newton, E. Gray, D.R. Taaffe, Exercise-induced myokines and their effect on prostate cancer, Nat. Rev. Urol. 18 (2021) 519–542.
[47] S. Looijaard, M.L. Te Lintel Hekkert, R.C.I. Wüst, R.H.J. Otten, C.G.M. Meskers, A. B. Maier, Pathophysiological mechanisms explaining poor clinical outcome of older cancer patients with low skeletal muscle mass, Acta Physiol. 231 (2021), e13516.
[48] A. Ruiz-Casado, A. Martín-Ruiz, L.M. Pérez, M. Provencio, C. Fiuza-Luces, A. Lucia, Exercise and the hallmarks of cancer, Trends Cancer 3 (2017) 423–441.
[49] C. Van den Eynde, J. Vriens, K. De Clercq, Transient receptor potential channel regulation by growth factors, Biochim. Biophys. Acta Mol. Cell Res. 1868 (2021), 118950.
[50] K. Kiselyov, R.L. Patterson, The integrative function of TRPC channels, Front. Biosci. 14 (2009) 45–58.
[51] I. Masgras, S. Carrera, P.J. de Verdier, P. Brennan, A. Majid, W. Makhtar, E. Tulchinsky, G.D.D. Jones, I.B. Roninson, S. Macip, Reactive oxygen species and mitochondrial sensitivity to oxidative stress determine induction of cancer cell death by p21, J. Biol. Chem. 287 (2012) 9845–9854.
[52] M. Ristow, K. Schmeisser, Mitohormesis: promoting health and lifespan by increased levels of reactive oxygen species (ROS), Dose Response 12 (2014) 288–341.
[53] K. Tanaka, K. Sato, T. Yoshida, T. Fukuda, K. Hanamura, N. Kojima, T. Shirao, T. Yanagawa, H. Watanabe, Evidence for cell density affecting C2C12 myogenesis: possible regulation of myogenesis by cell–cell communication, Muscle Nerve 44 (2011) 968–977.
[54] J. Lee, J. Park, Y.H. Kim, N.H. Lee, K.-M. Song, Irisin promotes C2C12 myoblast proliferation via ERK-dependent CCL7 upregulation, PLoS One 14 (2019), e0222559.
[55] S.E. Mulder, A. Dasgupta, R.J. King, J. Abrego, K.S. Attri, D. Murthy, S.K. Shukla, P. K. Singh, JNK signaling contributes to skeletal muscle wasting and protein turnover in pancreatic cancer cachexia, Cancer Lett. 491 (2020) 70–77.
[56] D.D. Sarbassov, L.G. Jones, C.A. Peterson, Extracellular signal-regulated kinase-1 and-2 respond differently to mitogenic and differentiative signaling pathways in myoblasts, Mol. Endocrinol. 11 (1997) 2038–2047.
[57] H. Aswad, A. Jalabert, S. Rome, Depleting extracellular vesicles from fetal bovine serum alters proliferation and differentiation of skeletal muscle cells in vitro, BMC Biotechnol. 16 (2016) 1–12.
[58] S.D. Dutta, T. Park, K. Ganguly, D.K. Patel, J. Bin, M.-C. Kim, K.-T. Lim, Evaluation of the sensing potential of stem cell-secreted proteins via a microchip device under electromagnetic field stimulation, ACS Appl. Bio Mater. 4 (2021) 6853–6864.
[59] Y. Jang, Y. Lee, S.M. Kim, Y.D. Yang, J. Jung, U. Oh, Quantitative analysis of TRP channel genes in mouse organs, Arch Pharm. Res. (Seoul) 35 (2012) 1823–1830.
[60] S. Crocetti, C. Beyer, S. Unternährer, T. Benavides Damm, G. Schade-Kampmann, M. Hebeisen, M. Di Berardino, J. Fröhlich, A. Franco-Obregón, Impedance flow cytometry gauges proliferative capacity by detecting TRPC1 expression, Cytometry 85 (2014) 525–536.
[61] C.Y. Matsumura, A.P. Taniguti, A. Pertille, H. Santo Neto, M.J. Marques, Stretch-activated calcium channel protein TRPC1 is correlated with the different degrees of the dystrophic phenotype in mdx mice, Am. J. Physiol. Cell Physiol. 301 (2011) C1344–C1350.
[62] J.F. Rolland, A. De Luca, R. Burdi, F. Andreetta, P. Confalonieri, D. Conte Camerino, Overactivity of exercise-sensitive cation channels and their impaired modulation by IGF-1 in mdx native muscle fibers: beneficial effect of pentoxifylline, Neurobiol. Dis. 24 (2006) 466–474.
[63] B.T. Zhang, N.P. Whitehead, O.L. Gervasio, T.F. Reardon, M. Vale, D. Fatkin, A. Dietrich, E.W. Yeung, D.G. Allen, Pathways of Ca^{2+} entry and cytoskeletal damage following eccentric contractions in mouse skeletal muscle, J. Appl. Physiol. 1985 (112) (2012) 2077–2086.
[64] P.C. Kerstein, B.T. Jacques-Fricke, J. Rengifo, B.J. Mogen, J.C. Williams, P. A. Gottlieb, F. Sachs, T.M. Gomez, Mechanosensitive TRPC1 channels promote calpain proteolysis of talin to regulate spinal axon outgrowth, J. Neurosci. 33 (2013) 273–285.
[65] O.L. Gervásio, N.P. Whitehead, E.W. Yeung, W.D. Phillips, D.G. Allen, TRPC1 binds to caveolin-3 and is regulated by Src kinase - role in Duchenne muscular dystrophy, J. Cell Sci. 121 (2008) 2246–2255.
[66] T. Benavides Damm, S. Richard, S. Tanner, F. Wyss, M. Egli, A. Franco-Obregón, Calcium-dependent deceleration of the cell cycle in muscle cells by simulated microgravity, Faseb. J. 27 (2013) 2045–2054.
[67] X. Tian, D. Wang, M. Zha, X. Yang, X. Ji, L. Zhang, X. Zhang, Magnetic field direction differentially impacts the growth of different cell types, Electromagn. Biol. Med. 37 (2018) 114–125.
[68] P.J. Hore, H. Mouritsen, The radical-pair mechanism of magnetoreception, Annu. Rev. Biophys. 45 (2016) 299–344.
[69] G.C. Nordmann, T. Hochstoeger, D.A. Keays, Magnetoreception-A sense without a receptor, PLoS Biol. 15 (2017), e2003234.
[70] D. Kattnig, E. Evans, V. Déjean, C. Dodson, M. Wallace, S. Mackenzie, C. Timmel, P. Hore, Chemical amplification of magnetic field effects relevant to avian magnetoreception, Nat. Chem. 8 (2016) 384–391.
[71] R.J. Usselman, C. Chavarriaga, P.R. Castello, M. Procopio, T. Ritz, E.A. Dratz, D. J. Singel, C.F. Martino, The quantum biology of reactive oxygen species partitioning impacts cellular bioenergetics, Sci. Rep. 6 (2016) 1–6.
[72] R.J. Usselman, I. Hill, D.J. Singel, C.F. Martino, Spin biochemistry modulates reactive oxygen species (ROS) production by radio frequency magnetic fields, PLoS One 9 (2014), e93065.
[73] Y. Gao, P. Wen, R.T. Cardé, H. Xu, Q. Huang, In addition to cryptochrome 2, magnetic particles with olfactory co-receptor are important for magnetic orientation in termites, Commun. Biol. 4 (2021) 1–12.
[74] J.A. Butterwick, J. Del Mármol, K.H. Kim, M.A. Kahlson, J.A. Rogow, T. Walz, V. Ruta, Cryo-EM structure of the insect olfactory receptor Orco, Nature 560 (2018) 447–452.
[75] F. Zufall, A.I. Domingos, The structure of Orco and its impact on our understanding of olfaction, J. Gen. Physiol. 150 (2018) 1602–1605.
[76] L. Mukunda, S. Lavista-Llanos, B.S. Hansson, D. Wicher, Dimerisation of the Drosophila odorant coreceptor Orco, Front. Cell. Neurosci. 8 (2014) 261.
[77] M. Lowe, J. Lage, E. Paatela, D. Munson, R. Hostager, C. Yuan, N. Katoku-Kikyo, M. Ruiz-Estevez, Y. Asakura, J. Staats, Cry2 is critical for circadian regulation of myogenic differentiation by Bclaf1-mediated mRNA stabilization of cyclin D1 and Tmem176b, Cell Rep. 22 (2018) 2118–2132.
[78] M.E. Vaughan, M. Wallace, M.K. Handzlik, A.B. Chan, C.M. Metallo, K.A. Lamia, Cryptochromes suppress HIF1α in muscles, iScience 23 (2020), 101338.
[79] J.F. Margiotta, M.J. Howard, Cryptochromes mediate intrinsic photomechanical transduction in avian iris and somatic striated muscle, Front. Physiol. 11 (2020) 128.
[80] E. Contreras, A.P. Nobleman, P.R. Robinson, T.M. Schmidt, Melanopsin phototransduction: beyond canonical cascades, J. Exp. Biol. 224 (2021).
[81] P.B. Detwiler, Phototransduction in retinal ganglion cells, Yale J. Biol. Med. 91 (2018) 49–52.
[82] M.N. Moraes, L.V.M. de Assis, I. Provencio, A.M.L. Castrucci, Opsins outside the eye and the skin: a more complex scenario than originally thought for a classical light sensor, Cell Tissue Res. 385 (2021) 519–538.
[83] X. Chen, G. Sooch, I.S. Demaree, F.A. White, A.G. Obukhov, Transient receptor potential canonical (TRPC) channels: then and now, Cells 9 (2020).
[84] M. Guescini, S. Maggio, P. Ceccaroli, M. Battistelli, G. Annibalini, G. Piccoli, P. Sestili, V. Stocchi, Extracellular vesicles released by oxidatively injured or intact C2C12 myotubes promote distinct responses converging toward myogenesis, Int. J. Mol. Sci. 18 (2017) 2488.
[85] P.E.M. de Castilla, L. Tong, C. Huang, A.M. Sofias, G. Pastorin, X. Chen, G. Storm, R.M. Schiffelers, J.-W. Wang, Extracellular vesicles as a drug delivery system: a systematic review of preclinical studies, Adv. Drug Deliv. Rev. 175 (2021), 113801.